A SWITCHING-PARAMETER ALGORITHM FOR FINDING MULTIPLE SOLUTIONS OF NONLINEAR RESISTIVE CIRCUITS

by

L. O. Chua and A. Ushida

Memorandum No. ERL-M497

February 1975

ELECTRONICS RESEARCH LABORATORY

College of Engineering
University of California, Berkeley
94720

A SWITCHING-PARAMETER ALGORITHM FOR FINDING MULTIPLE SOLUTIONS OF NONLINEAR RESISTIVE CIRCUITS†

L. O. Chua and A. Ushida

ABSTRACT

An efficient algorithm for finding multiple solutions of a system of nonlinear algebraic equations is presented. This algorithm consists of solving an associated system of first order nonlinear differential equations whose independent variable may be switched from one variable to another during each integration step. The choice of the forward Euler predictor and Newton-Raphson corrector for integrating the differential equations leads to an extremely efficient method for implementing this switching-parameter algorithm. This approach involves only the recursive solution of an associated system of linear algebraic equations and can be easily programmed. The switching-parameter algorithm can also be used to derive the driving-point or transfer characteristic curve of multivalued resistive nonlinear networks.

L. O. Chua is with the Department of Electrical Engineering and Computer Sciences, University of California, Berkeley, California 94720.

A. Ushida is with the Department of Electrical Engineering, Technical College of Tokushima University, Tokushima, Japan.

† Research sponsored by the Joint Services Electronics Program Contract F44620-71-C-0087 and the National Science Foundation Grant GK-32236X1.

I. INTRODUCTION

One of the most basic yet unsolved problems in the analysis and design of nonlinear circuits [1] and systems [2] is that of finding the set of all solutions of a "well-posed"[1] system of nonlinear equations

$$\begin{aligned} f_1(x_1,x_2,\ldots,x_n) &= 0 \\ f_2(x_1,x_2,\ldots,x_n) &= 0 \\ &\vdots \\ f_n(x_1,x_2,\ldots,x_n) &= 0 \end{aligned} \tag{1}$$

over some compact domain $D \subset \mathbb{R}^n$. The classical Newton-Raphson algorithm is not applicable since it generally converges only if the initial guess is close to a solution, and no algorithm is known for choosing an appropriate set of initial guesses [3].

Several methods for finding multiple solutions have been proposed in the last few years, but as yet no efficient and satisfactory method is available. The piecewise-linear method proposed by Chua [4] is capable of finding all solutions, but it is applicable only for solving equations of the type assocaited with circuits containing uncoupled piecewise-linear resistors. The recent algorithm due to Chien and Kuh [5] is applicable to an arbitrary system of piecewise-linear equations, but there is no guarantee that all solutions will be found in a finite number of iterations.

Another class of algorithms for finding solutions of $\underset{\sim}{f}(\underset{\sim}{x}) = \underset{\sim}{0}$ consists of numerically integrating some associated system of nonlinear

[1] A system of equations $\underset{\sim}{f}(\underset{\sim}{x}) = \underset{\sim}{0}$ is said to be well-posed in this paper if it possesses at least one solution and all solutions are isolated.

ordinary differential equations in the normal form [6-10]. Among these algorithms, only Shinohara [10], Branin [11], and Chao's [12] algorithms have been devised specifically for finding the multiple solutions. Shinohara and Chao's algorithms[2] consist of numerically integrating for a particular trajectory which coincides with the intersection of the (n-1) surfaces defined by the first (n-1) equations $f_i(x_1,x_2,\ldots,x_n) = 0$, $i = 1,2,\ldots,n-1$. When the points on this trajectory are substituted into the remaining n-th equation $f_n(x_1,x_2,\ldots,x_n) = 0$, a solution to $\underset{\sim}{f}(\underset{\sim}{x}) = \underset{\sim}{0}$ is found whenever the function $f_n(\cdot)$ changes sign. Two difficulties may be identified with this approach: first, an initial point on a particular trajectory must first be found, say by a Newton-Raphson algorithm. This preliminary step could itself be rather time consuming, and second, the solution may lie on more than one distinct trajectory, in which case, only those solutions associated with one particular trajectory will be found.

Although the trajectories associated with Shinohara and Chao's methods are identical, Chao's method is actually a modified version of Branin's method wherein each solution to $\underset{\sim}{f}(\underset{\sim}{x}) = \underset{\sim}{0}$ is also a singular point of the associated differential equations. Since an infinite amount of time is required in theory for a trajectory to arrive at a singular point, each solution can only be determined approximately -- after some finite integration time interval whose length could vary widely depending on how fast the trajectory approaches the singular point. Unlike Shinohara

[2] Although the differential equations associated with Shinohara and Chao's algorithm are different, the respective trajectories being sought are identical. Although theoretically more elegant, Shinohara's method is much more time consuming compared to Chao's method because it requires the evaluation of the determinants of "n" (n-1) x (n-1) matrices per integration step and is therefore inefficient when "n" is large.

and Chao, Branin's method does not require any prior initial guess and is therefore self-starting. However, Branin's emthod is rather inefficient because each time step requires the computation of the determinant of "n" n x n matrices. Moreover, extraneous singular points which could be mistaken for solutions are usually generated.

In this paper, we propose yet another approach -- the switching-parameter algorithm -- for finding multiple solutions by integrating an associated system of differential equations. Though not flawless, our algorithm is numerically efficient and is applicable to a relatively large class of equations. It is also particularly suited for finding multivalued driving-point and transfer characteristic curves of resistive nonlinear circuits. A detailed derivation and implementation of this algorithm will be given in Sections II and III. An analysis of the properties of this algorithm will be presented in Section IV and some applications of this algorithm to the analysis of resistive nonlinear networks having multiple solutions will be given in Section V. Finally, some difficulties that could arise with this algorithm will be described in the concluding Section VI.

II. THE SWITCHING PARAMETER APPROACH

Consider a system of "n" well-posed algebraic equations

$$\underset{\sim}{f}(\underset{\sim}{x}) = \underset{\sim}{0} \tag{2}$$

in n unknowns $\underset{\sim}{x} \triangleq [x_1, x_2, \ldots, x_n]^t$, where $\underset{\sim}{f}(\cdot)$: $\mathbb{R}^n \to \mathbb{R}^n$ is a C^2 function. Suppose we introduce a parameter $\rho \in \mathbb{R}^1$ and define an augmented system of "n" equations

$$\hat{\underset{\sim}{f}}(\underset{\sim}{x}, \rho) = \underset{\sim}{0} \tag{3}$$

in (n+1) unknowns $[\underset{\sim}{x}, \rho] \triangleq [x_1, x_2, \ldots, x_n, \rho]^t$ such that Eq. (3) possesses the following three properties:

(1) At some initial value $\rho = \rho_0$, a solution $\underset{\sim}{x}_0$ of Eq. (3) is known, a priori; i.e.,

$$\hat{\underset{\sim}{f}}(\underset{\sim}{x}_0, \rho_0) = \underset{\sim}{0} \tag{4}$$

(2) At some value $\rho^* \neq \rho_0$, Eq. (3) reduces identically to Eq. (2); namely,

$$\hat{\underset{\sim}{f}}(\underset{\sim}{x}, \rho^*) = \underset{\sim}{f}(\underset{\sim}{x}) = 0 \tag{5}$$

(3) For each $\rho \in \mathbb{R}^1$, $\hat{\underset{\sim}{f}}(\underset{\sim}{x}, \rho) = 0$ is a well-posed system of equations.

There exist many methods for constructing an augmented equation with the preceding properties. In the case of nonlinear circuits containing passive resistive elements -- such as resistors, diodes and transistors -- and a battery (or several batteries with identical terminal voltage E), we can simply choose $\rho = E$, and observe that the solution voltages are equal to zero when $E = 0$.

In the general case, we can always define the augmented system [7]

$$\hat{\underset{\sim}{f}}(\underset{\sim}{x},\rho) \triangleq \underset{\sim}{f}(\underset{\sim}{x}) + (\rho-1)\ \underset{\sim}{f}(\underset{\sim}{x}_0) = \underset{\sim}{0} \tag{6}$$

where $\underset{\sim}{x}_0$ is any initial guess. Observe that $\hat{\underset{\sim}{f}}(\underset{\sim}{x},0) = \underset{\sim}{f}(\underset{\sim}{x}) - \underset{\sim}{f}(\underset{\sim}{x}_0)$ has an obvious solution at $\underset{\sim}{x} = \underset{\sim}{x}_0$, and $\hat{\underset{\sim}{f}}(\underset{\sim}{x},1) = \underset{\sim}{f}(\underset{\sim}{x})$. Hence Eq. (6) satisfies Eqs. (4) and (5) with $\rho_0 = 0$ and $\rho^* = 1$. Needless to say, there exist many other augmented systems having similar properties.

Since the augmented system has one more unknown than there are equations, there exists in general a continuum of points which satisfies Eq. (3). Since our equations are assumed to be well-posed, all solutions of Eq. (3) are assumed to be isolated for all values of ρ. Geometrically, the solutions of the augmented system can be interpreted as shown in Fig. 1 as a collection of space curves in the $(x_1 - x_2 - \ldots - x_n - \rho)$ - space. In this hypothetical example there are two initial vectors $\underset{\sim}{x}_0^{(1)}$ and $\underset{\sim}{x}_0^{(2)}$ lying within the compact subset $D(\rho_0)$ of the hyperplane $\rho = \rho_0$. The corresponding solutions are located at the intersections of these space curves with the hyperplane $\rho = \rho^*$; namely, $\underset{\sim}{x}^{*(1)}, \underset{\sim}{x}^{*(2)}, \ldots, \underset{\sim}{x}^{*(6)}$ within the compact subset $D(\rho^*)$. It follows from this observation that any algorithm which is capable of tracing these space curves efficiently can be used to find the multiple solutions of Eq. (2). Observe also that if there is more than one disconnected solution branch, such as the two branches shown in Fig. 1, then only those solutions lying on that particular branch which passes through the given initial guess $\underset{\sim}{x}_0$ will be found. Although no algorithm is yet available for finding all solution branches, we will show via an example in section V that solutions lying on distinct branches of solution curves

can often be found by choosing several uniformly spaced initial guesses $\underset{\sim}{x}_0^{(1)}, \underset{\sim}{x}_0^{(2)}, \ldots, \underset{\sim}{x}_0^{(k)}$ on the boundary of some prescribed compact domain $D \subset \mathbb{R}^n$. The main contribution of this paper is to propose an efficient algorithm for tracing the solution curve associated with the augmented system.

Let $\Gamma(\underset{\sim}{x}_0)$ denote a solution curve of Eq. (3) passing through some prescribed initial guess $\underset{\sim}{x}_0$. Such a space curve can always be represented by a system of parametric equations

$$\left.\begin{aligned} x_1 &= x_1(s) \\ x_2 &= x_2(s) \\ &\vdots \\ x_n &= x_n(s) \\ \rho &= \rho(s) \end{aligned}\right\} \tag{7}$$

where s is some suitable parameter. For example, we can always choose s to be the arc-length measured from the initial guess $\underset{\sim}{x}_0$. This choice, however, would require an enormous amount of computation if n is large. To overcome this objection, we could choose another parameter which exhibits a one-to-one correspondence with the arc-length over some appropriately chosen interval, but which is computationally more efficient. For example, we could partition the solution curve into several connected segments, each segment being parametrized separately. In particular, we could project the solution curve onto each of the axes $x_1, x_2, \ldots, x_n$, and ρ, and then parametrize each segment with the projection map onto some appropriately chosen axis. To be specific, let Γ_j and Γ_k denote two adjacent segments of the solution curve and let $(\bar{\underset{\sim}{x}}, \bar{\rho})$ denote the coordinates of the end point of Γ_j, or the beginning point of Γ_k.

Then a simple parameter to choose for tracing Γ_k is $s = \pm(x_i - \bar{x}_i)$, for some i, or $s = \pm(\rho - \bar{\rho})$, so long as the value of x_i, or ρ, is restricted to lie within the projected interval for segment Γ_k. The sign is chosen in such a way that the solution curve is continuously traced along the same direction. For example, consider the solution curve in the ρ - vs. - x plane in Fig. 2, where the initial guess is located at (x_0,ρ_0) and where the solutions are located at Q_1: $(x^{*(1)},\rho^*)$, Q_2: $(x^{*(2)},\rho^*)$ and Q_3: $(x^{*(3)},\rho^*)$. The projection of this solution curve onto the x-axis is given by the interval $[x_a,x_g]$, while that onto the ρ-axis is given by the interval $[\rho_c,\rho_e]$. Hence, we can partition the solution curve into four segments and choose our parameter s as follows:

segment 1: $s = (x-x_b)$ for $x_b \leq x \leq x_f$

segment 2: $s = -(\rho-\rho_f)$ for $\rho_h \leq \rho \leq \rho_f$

segment 3: $s = -(x-x_h)$ for $x_i \leq x \leq x_h$

segment 4: $s = -(\rho-\rho_i)$ for $\rho_b \leq s \leq \rho_i$

Observe that $[x_b,x_f] \subset [x_a,x_g]$, $[\rho_h,\rho_f] \subset [\rho_c,\rho_e]$, $[x_i,x_h] \subset [x_a,x_g]$, and $[\rho_b,\rho_i] \subset [\rho_c,\rho_e]$.

Needless to say, there is an infinite number of ways to partition the solution curve. However, to avoid going outside the projected interval on each axis, a good strategy will be to choose the parameter s at each point on the solution curve to be that variable $x_k \in \{x_1,x_2,\ldots x_n,\rho\}$ which changes most rapidly. For example, at point (e) on the curve, we choose $s = (x-x_e)$ since $|\Delta x| > |\Delta\rho|$ about a small neighborhood of point (e). On the other hand, we choose $s = (\rho-\rho_g)$ at point (g) since $|\Delta\rho| > |\Delta x|$ about a small neighborhood of point (g). If we

adopt this strategy for each point on the solution curve, then we are guaranteed that

$$\left|\frac{dx_i}{ds}\right| \leq 1, \quad i = 1,2,\ldots,n \tag{8}$$

and

$$\left|\frac{d\rho}{ds}\right| \leq 1 \tag{9}$$

where the equality sign is attained only if $s = \pm(x_i - \bar{x}_i)$, or $s = \pm(\rho - \bar{\rho})$, where $\bar{x}_i$ or $\bar{\rho}$ is associated with the beginning point of the segment in question. To determine the precise rate of change of x_i and ρ with respect to the parameter s, let us differentiate both sides of $\hat{f}_i(\underset{\sim}{x},\rho) = 0$ with respect to s:

$$\sum_{j=1}^{n} \frac{\partial \hat{f}_i(\underset{\sim}{x},\rho)}{\partial x_j} \frac{dx_j}{ds} + \frac{\partial \hat{f}_i(\underset{\sim}{x},\rho)}{\partial \rho} \frac{d\rho}{ds} = 0, \quad i = 1,2,\ldots,n \tag{10}$$

Now at any point $(\underset{\sim}{x},\rho)$ on the solution curve, choose $s = \pm(x_k - \bar{x}_k)$ such that Eqs. (8) and (9) are satisfied. In other words, choose the index "k" such that the solution curve at $(\underset{\sim}{x},\rho)$ changes most rapidly in the direction of the coordinate axis x_k. The plus or the minus sign will be chosen later in the integration process to assure that the solution curve is always traced in the same direction. Substituting $dx_k/ds = \pm 1$ into Eq. (10) and rearranging terms, we obtain the following system of associated differential equations:

$$\begin{bmatrix} \frac{dx_1}{ds} \\ \frac{dx_2}{ds} \\ \vdots \\ \frac{dx_{k-1}}{ds} \\ \frac{dx_{k+1}}{ds} \\ \vdots \\ \frac{dx_n}{ds} \\ \frac{d\rho}{ds} \end{bmatrix} = \begin{bmatrix} \frac{\partial \hat{f}_1(\underset{\sim}{x},\rho)}{\partial x_1} & \frac{\partial \hat{f}_1(\underset{\sim}{x},\rho)}{\partial x_2} & \cdots & \frac{\partial \hat{f}_1(\underset{\sim}{x},\rho)}{\partial x_{k-1}} & \frac{\partial \hat{f}_1(\underset{\sim}{x},\rho)}{\partial x_{k+1}} & \cdots & \frac{\partial \hat{f}_1(\underset{\sim}{x},\rho)}{\partial x_n} & \frac{\partial \hat{f}_1(\underset{\sim}{x},\rho)}{\partial \rho} \\ \frac{\partial \hat{f}_2(\underset{\sim}{x},\rho)}{\partial x_1} & \frac{\partial \hat{f}_2(\underset{\sim}{x},\rho)}{\partial x_2} & \cdots & \frac{\partial \hat{f}_2(\underset{\sim}{x},\rho)}{\partial x_{k-1}} & \frac{\partial \hat{f}_2(\underset{\sim}{x},\rho)}{\partial x_{k+1}} & \cdots & \frac{\partial \hat{f}_2(\underset{\sim}{x},\rho)}{\partial x_n} & \frac{\partial \hat{f}_2(\underset{\sim}{x},\rho)}{\partial \rho} \\ \vdots & & & \vdots & \vdots & & \vdots & \vdots \\ \frac{\partial \hat{f}_{n-1}(\underset{\sim}{x},\rho)}{\partial x_1} & \frac{\partial \hat{f}_{n-1}(\underset{\sim}{x},\rho)}{\partial x_2} & \cdots & \frac{\partial \hat{f}_{n-1}(\underset{\sim}{x},\rho)}{\partial x_{k-1}} & \frac{\partial \hat{f}_{n-1}(\underset{\sim}{x},\rho)}{\partial x_{k+1}} & \cdots & \frac{\partial \hat{f}_{n-1}(\underset{\sim}{x},\rho)}{\partial x_n} & \frac{\partial \hat{f}_{n-1}(\underset{\sim}{x},\rho)}{\partial \rho} \\ \frac{\partial \hat{f}_n(\underset{\sim}{x},\rho)}{\partial x_1} & \frac{\partial \hat{f}_n(\underset{\sim}{x},\rho)}{\partial x_2} & \cdots & \frac{\partial \hat{f}_n(\underset{\sim}{x},\rho)}{\partial x_{k-1}} & \frac{\partial \hat{f}_n(\underset{\sim}{x},\rho)}{\partial x_{k+1}} & \cdots & \frac{\partial \hat{f}_n(\underset{\sim}{x},\rho)}{\partial x_n} & \frac{\partial \hat{f}_n(\underset{\sim}{x},\rho)}{\partial \rho} \end{bmatrix}^{-1} \begin{bmatrix} \mp \frac{\partial \hat{f}_1(\underset{\sim}{x},\rho)}{\partial x_k} \\ \mp \frac{\partial \hat{f}_2(\underset{\sim}{x},\rho)}{\partial x_k} \\ \vdots \\ \mp \frac{\partial \hat{f}_n(\underset{\sim}{x},\rho)}{\partial x_k} \end{bmatrix} \tag{11}$$

The inverse matrix in Eq. (11) is well-defined in view of Eq. (8) and (9). (See Proposition 1 of Sec. IV.) Observe that Eq. (11) is the differential equation governing the solution curve of Eq. (3). Consequently, the trajectory through the initial guess $(\underset{\sim}{x}_0, \rho_0)$ is precisely the solution curve of Eq. (3). It must be emphasized that since the parameter $s = \pm(x_k - \bar{x}_k)$ could change from point to point on the solution curve, the k-th column in the matrix may change position from one integration step to another. In other words, Eq. (11) actually represents (n+1) "distinct" systems of equations.

III. PRACTICAL IMPLEMENTATION OF THE SWITCHING-PARAMETER APPROACH

Since Eq. (11) could conceivably switch from one system to another after each integration step, a single-step integration algorithm is preferred over the more efficient multi-step algorithms [13]. The approach to be described in this section uses the Forward Euler algorithm to predict an initial guess near the solution curve. The Newton-Raphson algorithm is then used as a corrector to zero in to an accurate solution point. Two Newton iterations per time step have been found to be more than adequate for this purpose. This Forward Euler Predictor-Newton Raphson Corrector algorithm can be streamlined and implemented very efficiently by solving an alternate but equivalent form of Eq. (11). To derive this equation, observe that along the solution curve, Eqs. (3) and (10) may be combined into one equation; namely,

$$\frac{d\hat{\underset{\sim}{f}}(\underset{\sim}{x},\rho)}{ds} = \left[\frac{\partial\hat{\underset{\sim}{f}}(\underset{\sim}{x},\rho)}{\partial\underset{\sim}{x}} \quad \frac{\partial\hat{\underset{\sim}{f}}(\underset{\sim}{x},\rho)}{\partial\rho}\right]\begin{bmatrix}\frac{d\underset{\sim}{x}}{ds}\\ \\ \frac{d\rho}{ds}\end{bmatrix} = -c\hat{\underset{\sim}{f}}(\underset{\sim}{x},\rho) \qquad (12)$$

where c is an arbitrary positive constant.

Solving Eq. (12) for $\hat{\underset{\sim}{f}}(\cdot)$, we have

$$\hat{\underset{\sim}{f}}(\underset{\sim}{x}(s),\rho(s)) = \hat{\underset{\sim}{f}}(\underset{\sim}{x}^{(j)},\rho^{(j)})e^{-cs} \qquad (13)$$

where $\underset{\sim}{f}(\underset{\sim}{x}^{(j)},\rho^{(j)})$ could be interpreted as an error vector at the j-th integration time step. Observe that adding the term $-c\hat{\underset{\sim}{f}}(\underset{\sim}{x},\rho)$ in Eq. (12) has the desirable effect of damping out the local truncation error. Consequently, instead of integrating Eq. (11), let us focus on Eq. (12). As it stands, Eq. (12) consists of a system of "n" equations in (n+1) variables. To these, however, we add the equation

$$\text{sgn}\left(\frac{dx_k}{ds}\right)\frac{dx_k}{ds} = 1 \tag{14}$$

where $s = \pm (x_k - \bar{x}_k)$ is chosen by the same recipe as before. Eqs. (12) and (14) can be expanded as follows:

$$\begin{bmatrix} \frac{\partial \hat{f}_1}{\partial x_1} & \frac{\partial \hat{f}_1}{\partial x_2} & \cdots & \frac{\partial \hat{f}_1}{\partial x_k} & \cdots & \frac{\partial \hat{f}_1}{\partial x_n} & \frac{\partial \hat{f}_1}{\partial \rho} \\ \frac{\partial \hat{f}_2}{\partial x_1} & \frac{\partial \hat{f}_2}{\partial x_2} & \cdots & \frac{\partial \hat{f}_2}{\partial x_k} & \cdots & \frac{\partial \hat{f}_2}{\partial x_n} & \frac{\partial \hat{f}_2}{\partial \rho} \\ \vdots & \vdots & & \vdots & & \vdots & \vdots \\ \frac{\partial \hat{f}_n}{\partial x_1} & \frac{\partial \hat{f}_n}{\partial x_2} & \cdots & \frac{\partial \hat{f}_n}{\partial x_k} & \cdots & \frac{\partial \hat{f}_n}{\partial x_n} & \frac{\partial \hat{f}_n}{\partial \rho} \\ 0 & 0 & \cdots & \text{sgn}\left(\frac{dx_k}{ds}\right) & \cdots & 0 & 0 \end{bmatrix} \begin{bmatrix} \frac{dx_1}{ds} \\ \frac{dx_2}{ds} \\ \vdots \\ \frac{dx_n}{ds} \\ \frac{d\rho}{ds} \end{bmatrix} = \begin{bmatrix} -c\hat{f}_1(\underset{\sim}{x},\rho) \\ -c\hat{f}_2(\underset{\sim}{x},\rho) \\ \vdots \\ -c\hat{f}_n(\underset{\sim}{x},\rho) \\ 1 \end{bmatrix} \tag{15}$$

Now applying the Forward Euler algorithm to Eq. (15) with a step size h, we obtain

$$\begin{bmatrix} \frac{\partial \hat{f}_1}{\partial x_1} & \frac{\partial \hat{f}_1}{\partial x_2} & \cdots & \frac{\partial \hat{f}_1}{\partial x_k} & \cdots & \frac{\partial \hat{f}_1}{\partial x_n} & \frac{\partial \hat{f}_1}{\partial \rho} \\ \frac{\partial \hat{f}_2}{\partial x_1} & \frac{\partial \hat{f}_2}{\partial x_2} & \cdots & \frac{\partial \hat{f}_2}{\partial x_k} & \cdots & \frac{\partial \hat{f}_2}{\partial x_n} & \frac{\partial \hat{f}_2}{\partial \rho} \\ \vdots & \vdots & & \vdots & & \vdots & \vdots \\ \frac{\partial \hat{f}_n}{\partial x_1} & \frac{\partial \hat{f}_n}{\partial x_2} & \cdots & \frac{\partial \hat{f}_n}{\partial x_k} & \cdots & \frac{\partial \hat{f}_n}{\partial x_n} & \frac{\partial \hat{f}_n}{\partial \rho} \\ 0 & 0 & \cdots & \text{sgn}\left(\frac{dx_k}{ds}\right) & \cdots & 0 & 0 \end{bmatrix} \begin{bmatrix} x_1^{(j+1)} - x_1^{(j)} \\ x_2^{(j+1)} - x_2^{(j)} \\ \vdots \\ x_n^{(j+1)} - x_n^{(j)} \\ \rho^{(j+1)} - \rho^{(j)} \end{bmatrix} = -hc \begin{bmatrix} \hat{f}_1(\underset{\sim}{x}^{(j)},\rho^{(j)}) \\ \hat{f}_2(\underset{\sim}{x}^{(j)},\rho^{(j)}) \\ \vdots \\ \hat{f}_n(\underset{\sim}{x}^{(j)},\rho^{(j)}) \\ -\frac{1}{c} \end{bmatrix} \tag{16}$$

where $\frac{\partial f_i}{\partial x_j}$ and $\frac{\partial f_i}{\partial \rho}$ are evaluated at $\underset{\sim}{x} = x^{(j)}$ and $\rho = \rho^{(j)}$.

Since c is an arbitrary constant, let us choose $c = \frac{1}{h}$ and rewrite Eq. (16) as follows:

$$\underset{\sim}{J}(\underset{\sim}{x}^{(j)},\rho^{(j)}) \begin{bmatrix} \underset{\sim}{x}^{(j+1)}-\underset{\sim}{x}^{(j)} \\ \rho^{(j+1)}-\rho^{(j)} \end{bmatrix} = -\underset{\sim}{\hat{f}}(\underset{\sim}{x}^{(j)},\rho^{(j)}) \tag{17}$$

$$\operatorname{sgn}\left(\frac{dx_k}{ds}\bigg|_{x_k=x_k^{(j+1)}}\right)\left[x_k^{(j+1)}-x_k^{(j)}\right] = h \tag{18}$$

where $\underset{\sim}{J}(\underset{\sim}{x}^{(j)},\rho^{(j)})$ is an n x (n+1) submatrix made up of the first n rows of the matrix shown in Eq. (16). Observe that the expression $\operatorname{sgn}\left(\frac{dx_k}{ds}\Big|_{x_k=x_k^{(j+1)}}\right)$ in Eq. (18) must be evaluated at $x_k=x_k^{(j+1)}$ and not at $x_k=x_k^{(j)}$ in order to ensure that the solution curve will always be traced in the correct direction; i.e., no portion of the solution curve already traced will be retraced. It follows from Eq.(18) that $h = |\Delta x_k^{(j+1)}|$, where x_k is that variable which exhibits the maximum variation during the preceding integration step; i.e.,

$$|\Delta x_k^{(j)}| = \max\{|\Delta x_1^{(j)}|, |\Delta x_2^{(j)}|, \ldots, |\Delta x_n^{(j)}|, |\Delta\rho^{(j)}|\} \tag{19}$$

where $\Delta x_i^{(j)} \triangleq x_i^{(j)} - x_i^{(j-1)}$ and $\Delta\rho^{(j)} \triangleq \rho^{(j)} - \rho^{(j-1)}$.

Observe that Eqs. (17) and (18) consist of a system of (n+1) <u>linear equations</u> in (n+1) unknowns $\underset{\sim}{x}^{(j+1)}$, $\rho^{(j+1)}$. Solving this system by Gaussian elimination, or by any other efficient linear equation solver, we obtain the value of $\underset{\sim}{x}^{(j+1)}$ and $\rho^{(j+1)}$ as <u>predicted</u> by the Forward Euler algorithm. To reduce the local truncation error, we correct this predicted value by setting $x_k^{(j+1)} = x_k^{(j)}+h$ in Eq. (3) and solve for the remaining variables $x_1^{(j+1)}, x_2^{(j+1)}, \ldots, x_{k-1}^{(j+1)}, x_{k+1}^{(j+1)}, \ldots, x_n^{(j+1)}, \rho^{(j+1)}$ using the Newton-Raphson algorithm with the predicted value as the

initial guess. Observe, however, that this procedure is equivalent to that of solving Eqs. (17) and (18) with $h = 0$! Hence, our Forward Euler Predictor-Newton-Raphson Corrector algorithm can be efficiently implemented on the same set of linear equations. We can now summarize our algorithm as follows:

Step 0. Choose an appropriate step size h. Set $\underset{\sim}{x}^{(0)} = \underset{\sim}{x}_0$ and $\rho^{(0)} = \rho_0$. Set $x_k^{(0)} = \rho$ so that the last row of the matrix in Eq. (16) is given by $\underset{\sim}{J}_{n+1}^{(0)} = [0,\ldots 0,1]^t$. Set $|\Delta x_k^{(0)}| = h$.

Comment. For the examples in this paper, the typical values of h vary from 0.05 to 0.1.

Step 1. Set $j = 0$.

Step 2. Solve Eqs. (17) and (18) for $\underset{\sim}{x}^{(j+1)}$ and $\rho^{(j+1)}$. If there is a unique solution[3], find Δx_k such that $|\Delta x_k^{(j+1)}| = \max \{|\Delta x_1^{(j+1)}|, \ldots |\Delta x_n^{(n+1)}|, |\Delta\rho|\}$ and go to Step 3. If there is no solution, find the index k so that columns $1,2,\ldots k-1,k+1,\ldots,n+1$ of $\underset{\sim}{J}^{(j)}$ are linearly independent. The column "k" can be detected without any extra computation by examining the row-echelon matrix resulting from the Gaussian elimination of the Eqs. (17)-(18). Switch from the parameter $x_k^{(j)}$ to $x_k^{(j+1)}$ corresponding to the new column "k" and go to Step 4.

Comment. The switching procedure can be mechanized by substituting $x_k^{(j+1)}$ into the expression $\operatorname{sgn}\left(\frac{dx_k}{ds}\Big|_{x_k=x_k^{(j+1)}}\right)$ from Eq. (18) and solving once again the up-dated Eqs. (17)-(18) for $\underset{\sim}{x}^{(j+1)}$ and $\rho^{(j+1)}$.

Step 3. If $|\Delta x_k^{(j+1)}| = |\Delta x_k^{(j)}|$, go to Step 4.

---

[3] This algorithm is formulated under the assumption that the hypothesis of Proposition 1 in Section IV is satisfied. Hence, Eqs. (17) and (18) always have unique solutions except possibly when $j=0$, i.e. when the algorithm is initialized by arbitrarily setting $x_k^{(0)} = \rho$.

If $|\Delta x_k^{(j+1)}| \neq |\Delta x_k^{(j)}|$, switch from the parameter $x_k^{(j)}$ to $x_k^{(j+1)}$ and go to Step 4.

Comment. The values of $\underset{\sim}{x}^{(j+1)}$ and $\rho^{(j+1)}$ obtained from Steps 2 and 3 are the predicted values of $\underset{\sim}{x}$ and ρ at the $(j+1)$th integration step via the Forward Euler algorithm. The next steps will be to apply the Newton-Raphson corrector.

Step 4. Set $h = 0$ in Eq. (18). Substitute $\underset{\sim}{x}^{(j+1)}, \rho^{(j+1)}$ into Eq. (17) and solve for the first corrected value $\underset{\sim}{x}^{(j+1)'}, \rho^{(j+1)'}$. Observe that $(\underset{\sim}{x}^{(j+1)'}, \rho^{(j+1)'})$ represents the corrected value of $(\underset{\sim}{x}^{(j+1)}, \rho^{(j+1)})$ after one Newton-Raphson iteration.

Step 5. Repeat Step 4 with $\underset{\sim}{x}^{(j+1)} = \underset{\sim}{x}^{(j+1)'}$ and $\rho^{(j+1)} = \rho^{(j+1)'}$ and solve for the second corrected value $(\underset{\sim}{x}^{(j+1)''}, \rho^{(j+1)''})$. This value is that of $(\underset{\sim}{x}^{(j+1)}, \rho^{(j+1)})$ after two Newton-Raphson iterations.

Step 6. Set $j = j + 1$ and go to Step 2.

Comment. If necessary, Step 5 can be iterated until the local truncation error due to the Forward Euler algorithm is negligible. In most cases, however, two iterations are more than adequate.

The preceding algorithm is summarized in the flow chart shown in Fig.3. We will conclude this section with an example using this algorithm.

Example 1.

Find the solutions of the equations[4]

$$f_1(x_1,x_2,x_3) = a \sin(bx_1) \sin(bx_3) - x_2 = 0$$

---

[4] These equations are taken from Chao [12] where nine solutions have been found.

$$f_2(x_1,x_2,x_3) = c - dx_3 + ex_2 \sin(fx_3) - x_1 = 0$$
$$f_3(x_1,x_2,x_3) = g + hx_2 \sin(kx_1) - x_3 = 0$$

where $a = 2$, $b = 0.4\pi$, $c = 2.5$, $d = 1$, $e = 0.75$, $f = 2\pi$, $g = 1$, $h = 0.8$, and $k = 2\pi$. Recasting these equations into the form of Eq. (6) and using the switching parameter algorithm with $\underset{\sim}{x}_0 = (0,0,0)$ as the initial guess, we obtain the solution curve shown in Fig. 4. The nine points on this curve with $\rho = 1$ are the solutions. They are of course identical to those obtained earlier by Chao [12]. However, our algorithm is not only more efficient, but it also does not require the difficult task of finding an initial guess. In other words, our algorithm is self-starting.

IV. PROPERTIES OF THE SWITCHING ALGORITHM

The switching-parameter algorithm presented in the preceding section has been derived via a geometric and heuristic approach. Our objective in this section is to carry out a mathematical analysis of this algorithm. Our first proposition gives us a sufficient condition which guarantees that our associated differential equation is well-defined.

Proposition 1.

If the rank of the n x (n+1) Jacobian matrix of the vector-valued function $\hat{f}(x,\rho)$ from Eq. (3) is equal to n along the solution curve of the associated differential equation (11), then Step 2 of the preceding algorithm always gives a unique solution $(x^{(j+1)},\rho^{(j+1)})$.

Proof.

Along the solution curve of Eq. (11), Eq. (17) reduces to

$$\begin{bmatrix} \frac{\partial \hat{f}_1}{\partial x_1} & \frac{\partial \hat{f}_1}{\partial x_2} & \cdots & \frac{\partial \hat{f}_1}{\partial x_i} & \cdots & \frac{\partial \hat{f}_1}{\partial x_k} & \cdots & \frac{\partial \hat{f}_1}{\partial x_n} & \frac{\partial \hat{f}_1}{\partial \rho} \\ \frac{\partial \hat{f}_2}{\partial x_1} & \frac{\partial \hat{f}_2}{\partial x_2} & \cdots & \frac{\partial \hat{f}_2}{\partial x_i} & \cdots & \frac{\partial \hat{f}_2}{\partial x_k} & \cdots & \frac{\partial \hat{f}_2}{\partial x_n} & \frac{\partial \hat{f}_2}{\partial \rho} \\ \vdots & \vdots & & \vdots & & \vdots & & \vdots & \vdots \\ \frac{\partial \hat{f}_n}{\partial x_1} & \frac{\partial \hat{f}_n}{\partial x_2} & \cdots & \frac{\partial \hat{f}_n}{\partial x_i} & \cdots & \frac{\partial \hat{f}_n}{\partial x_k} & \cdots & \frac{\partial \hat{f}_2}{\partial x_n} & \frac{\partial \hat{f}_2}{\partial \rho} \\ 0 & 0 & \cdots & 0 & \cdots & \operatorname{sgn}\left(\frac{dx_k}{ds}\right) & \cdots & 0 & 0 \end{bmatrix} \begin{bmatrix} x_1^{(j+1)} - x_1^{(j)} \\ x_2^{(j+1)} - x_2^{(j)} \\ \vdots \\ x_n^{(j+1)} - x_n^{(j)} \\ \rho^{(j+1)} - \rho^{(j)} \end{bmatrix} = \begin{bmatrix} 0 \\ 0 \\ \vdots \\ 0 \\ h \end{bmatrix} \quad (20)$$

We initialize the algorithm by setting $x_k^{(0)} = \rho$. If the above matrix is nonsingular, a unique solution $(x^{(1)},\rho^{(1)})$ exists. If the matrix is singular but there exists a solution, then it is unique because $x_k^{(1)} = x_k^{(0)} + h$

is fixed. If there exists no solution, then since $\underset{\sim}{J}^{(0)}$ is of rank n, there is an index $\bar{k}$ such that the n columns $\{\underset{\sim}{J}_i^{(0)}\}_{i=1}^{n+1}$, $i \neq \bar{k}$ of the $n \times (n+1)$ Jacobian matrix constitute a linearly independent set. Hence, by switching parameter from $x_k^{(0)} = \rho$ to $x_k^{(0)} = x_{\bar{k}}^{(0)}$ and letting $x_{\bar{k}}^{(1)} = x_{\bar{k}}^{(0)} + h$, the values of all $x_i^{(1)}$, $i = 1,2,\ldots n+1$, $i \neq \bar{k}$ and $\rho^{(1)}$ are then uniquely determined. When $j > 1$, then since the rank of the Jacobian matrix is n, the solution $[\Delta\underset{\sim}{x},\Delta\rho]^{(j+1)} \triangleq [\underset{\sim}{x}^{(j+1)} - \underset{\sim}{x}^{(j)}, \rho^{(j+1)} - \rho^{(j)}]$ of the first n equations in Eq. (20) is a tangent vector to the curve $\mathcal{L}$ in the (n+1)-dimensional space defined by $f_i(\underset{\sim}{x},\rho) = 0$, $i = 1,2,\ldots n$. The last equation in Eq. (20) represents a hyperplane $\mathcal{H}$ defined by $x_k = x_k^{(j)} + h$. The set of solutions of Eq. (20) is the intersection $\mathcal{G}$ of $\mathcal{L}$ and $\mathcal{H}$. In particular, Eq. (20) has a unique solution if and only if $\mathcal{G}$ contains a single point. Since $|\Delta x_k| = |x_k^{(j+1)} - x_k^{(j)}| = \max\{|\Delta x_1|,\ldots|\Delta x_n|,|\Delta\rho|\} \neq 0$, the k-th component of the tangent vector to $\mathcal{L}$ at $[\underset{\sim}{x}^{(j)},\rho^{(j)}] \neq 0$. This implies that the tangent vector does not lie on the hyperplane and hence $\mathcal{G}$ contains only one point and therefore Eq. (20) has a unique solution. □

Observe that the hypothesis of Proposition 1 may be satisfied even for a function $\underset{\sim}{f}(\underset{\sim}{x})$ whose Jacobian does not have a full rank along the solution curve. This because the Jacobian matrix of $\underset{\sim}{f}(\underset{\sim}{x})$ is only one of "n" distinct n×n submatrices associated with the augmented function $\hat{\underset{\sim}{f}}(\underset{\sim}{x},\rho)$.

Our next proposition gives us a bound on the <u>local truncation error</u>

$$\varepsilon^{(j+1)} \triangleq \|\hat{\underset{\sim}{y}}^{(j+1)} - \underset{\sim}{y}^{(j+1)}\| \tag{21}$$

where

$$\hat{\underset{\sim}{y}}^{(j+1)} \triangleq [\hat{x}_1^{(j+1)},\hat{x}_2^{(j+1)},\ldots,\hat{x}_n^{(j+1)},\hat{\rho}^{(j+1)}]^t \tag{22}$$

and

$$\underset{\sim}{y}^{(j+1)} \triangleq [x_1^{(j+1)}, x_2^{(j+1)}, \ldots, x_n^{(j+1)}, \rho^{(j+1)}]^t \tag{23}$$

denote respectively the exact and the computed values of $x_1, x_2, \ldots, x_n$ and ρ at the $(j+1)$-th time step.

Proposition 2.

If the parametric equations $\hat{x}_1(s), \hat{x}_2(s), \ldots, \hat{x}_n(s)$, and $\hat{\rho}(s)$ of the solution curve have continuous second derivatives, and if the rank of the $n \times (n+1)$ Jacobian matrix of the vector-valued function $\hat{\underset{\sim}{f}}(\underset{\sim}{x}, \rho)$ from Eq. (3) is equal to n along the solution curve of Eq. (17), then the local truncation error $\varepsilon^{(j+1)}$ associated with the Forward Euler Predictor in Eq. (17) is bounded by

$$\varepsilon^{(j+1)} \leq \frac{h^2}{2} M,$$

where

$$M \triangleq \sqrt{\sum_{i=1}^{n} \sup \left(\frac{d^2 \hat{x}_i(s)}{ds^2}\right)^2 + \sup \left(\frac{d^2 \hat{\rho}(s)}{ds^2}\right)^2}, \tag{24}$$

where the supremum "sup" is taken over all values of s in the interval

$$\left.\begin{aligned} & s^{(j)} < s < s^{(j)} + h, \quad \text{if} \quad \operatorname{sgn} \left(\frac{dx_k}{ds}\Big|_{x_k = x_k^{(j)}}\right) > 0 \\ \text{or in the interval} \quad & \\ & s^{(j)} - h < s < s^{(j)}, \quad \text{if} \quad \operatorname{sgn} \left(\frac{dx_k}{ds}\Big|_{x_k = x_k^{(j)}}\right) < 0 \end{aligned}\right\} \tag{25}$$

Proof.

Since $\hat{x}_1(s), \hat{x}_2(s), \ldots, \hat{x}_n(s)$, and $\hat{\rho}(s)$ have continuous second

derivatives, we can apply Taylor's theorem with remainder [14] to each component of the vector $\hat{\underset{\sim}{y}}(s) \triangleq [\hat{x}_1(s), \hat{x}_2(s), \ldots, \hat{x}_n(s), \hat{\rho}(s)]^t$, about the point $\hat{\underset{\sim}{y}}^{(j)}(s^{(j)})$:

$$\hat{y}_i^{(j+1)} = \hat{y}_i + \left.\frac{d\hat{y}_i(s)}{ds}\right|_{s=s^{(j)}} h + \frac{h^2}{2} \left.\frac{d^2\hat{y}_i(s)}{ds^2}\right|_{s=\bar{s}_i}, \tag{26}$$

$$\left.\begin{aligned} &\text{where } s^{(j)} < \bar{s}_i < s^{(j)} + h, \quad \text{if } \operatorname{sgn}\left(\frac{dx_k}{ds}\right) > 0 \\ &\qquad s^{(j)} - h < \bar{s}_i < s^{(j)}, \quad \text{if } \operatorname{sgn}\left(\frac{dx_k}{ds}\right) < 0 . \end{aligned}\right\} \tag{27}$$

We can recast Eq. (26) into the following vector form

$$\hat{\underset{\sim}{y}}^{(j+1)} = \hat{\underset{\sim}{y}}^{(j)} + \left.\frac{d\hat{\underset{\sim}{y}}(s)}{ds}\right|_{s=s^{(j)}} h + \frac{h^2}{2} \left.\frac{d^2\hat{\underset{\sim}{y}}(s)}{ds^2}\right|_{s=\bar{\underset{\sim}{s}}} \tag{28}$$

where $s = \bar{\underset{\sim}{s}}$ is used to denote that $s = \bar{s}_i$ in $\hat{y}_i(s)$, $i = 1,2,\ldots,$ n+1. Now premultiply both sides of Eq. (28) by the Jacobian matrix $\hat{\underset{\sim}{J}}(\hat{\underset{\sim}{y}}^{(j)})$ of $\hat{\underset{\sim}{f}}(\underset{\sim}{x},\rho) = \hat{\underset{\sim}{f}}(\underset{\sim}{y})$, we obtain

$$\hat{\underset{\sim}{J}}(\hat{\underset{\sim}{y}}^{(j)})[\hat{\underset{\sim}{y}}^{(j+1)} - \hat{\underset{\sim}{y}}^{(j)}] = h\hat{\underset{\sim}{J}}(\hat{\underset{\sim}{y}}^{(j)}) \left.\frac{d\hat{\underset{\sim}{y}}(s)}{ds}\right|_{s=s^{(j)}} + \frac{h^2}{2} \hat{\underset{\sim}{J}}(y^{(j)}) \left.\frac{d^2\hat{\underset{\sim}{y}}(s)}{ds^2}\right|_{s=\bar{\underset{\sim}{s}}} . \tag{29}$$

Now since $\hat{\underset{\sim}{y}}^{(j)}$ is, by hypothesis, the exact solution, $\hat{\underset{\sim}{f}}(\hat{\underset{\sim}{y}}^{(j)}) = \underset{\sim}{0}$ and Eq. (15) simplifies to

$$\hat{\underset{\sim}{J}}(\hat{\underset{\sim}{y}}) \frac{d\hat{\underset{\sim}{y}}(s)}{ds} = \begin{bmatrix} 0 \\ \hline 1 \end{bmatrix} \tag{30}$$

Substituting Eq. (30) into Eq. (29), we obtain

$$\hat{\underset{\sim}{J}}(\hat{\underset{\sim}{y}}^{(j)})[\hat{\underset{\sim}{y}}^{(j+1)} - \hat{\underset{\sim}{y}}^{(j)}] = \begin{bmatrix} \underset{\sim}{0} \\ \hline h \end{bmatrix} + \frac{h^2}{2} \hat{\underset{\sim}{J}}(\hat{\underset{\sim}{y}}^{(j)}) \left.\frac{d^2\hat{\underset{\sim}{y}}(s)}{ds^2}\right|_{s=\bar{\underset{\sim}{s}}} \tag{31}$$

where $\hat{\underset{\sim}{J}}(\underset{\sim}{y})$ is computed from Eq. (17) with $\underset{\sim}{y}^{(j)} = \hat{\underset{\sim}{y}}^{(j)}$. Assuming that the preceding value $\underset{\sim}{y}^{(j)}$ is exact, then $\hat{\underset{\sim}{f}}(\hat{\underset{\sim}{y}}^{(j)}) = \underset{\sim}{0}$, and Eq. (17) simplifies to:

$$\hat{\underset{\sim}{J}}(\hat{\underset{\sim}{y}}^{(j)})[\underset{\sim}{y}^{(j+1)} - \hat{\underset{\sim}{y}}^{(j)}] = \begin{bmatrix} \underset{\sim}{0} \\ \cdots \\ h \end{bmatrix} \tag{32}$$

Subtracting Eq. (32) from Eq. (31), we obtain

$$\hat{\underset{\sim}{J}}(\hat{\underset{\sim}{y}}^{(j)})[\hat{\underset{\sim}{y}}^{(j+1)} - \underset{\sim}{y}^{(j+1)}] = \frac{h^2}{2}\, \hat{\underset{\sim}{J}}(\hat{\underset{\sim}{y}}^{(j)})\, \frac{d^2\hat{\underset{\sim}{y}}(s)}{ds^2}\bigg|_{s=\bar{s}} \tag{33}$$

Since $\hat{\underset{\sim}{J}}(\hat{\underset{\sim}{y}}^{(j)})$ is non-singular (proposition 1), we have

$$\hat{\underset{\sim}{y}}^{(j+1)} - \underset{\sim}{y}^{(j+1)} = \frac{h^2}{2}\, \frac{d^2\hat{\underset{\sim}{y}}(s)}{ds^2}\bigg|_{s=\bar{s}} \tag{34}$$

$$\therefore \|\hat{\underset{\sim}{y}}^{(j+1)} - \underset{\sim}{y}^{(j+1)}\| \leq \frac{h^2}{2} M\,. \tag{35}$$

when M is as defined in Eq. (24). □

Our next proposition applies only to the case where the augmented system is chosen as in Eq. (6) which we rewrite as

$$\hat{\underset{\sim}{f}}(\underset{\sim}{x}, \rho; \underset{\sim}{x}_0) \triangleq \underset{\sim}{f}(\underset{\sim}{x}) + (\rho - 1)\, \underset{\sim}{f}(\underset{\sim}{x}_0) = \underset{\sim}{0}, \tag{36}$$

in order to emphasize that Eq. (36) actually represents a continuum of distinct equations, each one identified by an arbitrary initial vector $\underset{\sim}{x}_0$. In other words, even though the solution curve of Eq. (36) will vary with the choice of $\underset{\sim}{x}_0$, they must all pass through the solutions of $\underset{\sim}{f}(\underset{\sim}{x}) = \underset{\sim}{0}$ at $\rho = 1$. Our next proposition asserts that these solution curves in fact cannot intersect anywhere else!

Proposition 3.

Let $\underset{\sim}{x}_0'$ and $\underset{\sim}{x}_0''$ be any two initial vectors which are independent in the sense that $\underset{\sim}{f}(\underset{\sim}{x}_0') \neq k\underset{\sim}{f}(\underset{\sim}{x}_0'')$, where k is an arbitrary constant. Let $\Gamma(\underset{\sim}{x}_0')$ and $\Gamma(\underset{\sim}{x}_0'')$ denote the respective solution curves plotted in the $\underset{\sim}{x}$-space with ρ as a parameter. Then any intersection $\bar{\underset{\sim}{x}}$ between $\Gamma(\underset{\sim}{x}_0')$ and $\Gamma(\underset{\sim}{x}_0'')$ must necessarily be a solution of $\underset{\sim}{f}(\underset{\sim}{x}) = \underset{\sim}{0}$.

Proof.

We will prove this proposition by contradiction. Suppose $\Gamma(\underset{\sim}{x}_0')$ and $\Gamma(\underset{\sim}{x}_0'')$ intersect at some point $\bar{\underset{\sim}{x}} \in \mathbb{R}^n$ such that $\underset{\sim}{f}(\bar{\underset{\sim}{x}}) \neq \underset{\sim}{0}$. Then

$$\hat{\underset{\sim}{f}}(\bar{\underset{\sim}{x}},\rho';\underset{\sim}{x}_0') \triangleq \underset{\sim}{f}(\bar{\underset{\sim}{x}}) + (\rho'-1)\,\underset{\sim}{f}(\underset{\sim}{x}_0') = \underset{\sim}{0},\ \rho' \neq 1 \tag{37}$$

and

$$\hat{\underset{\sim}{f}}(\bar{\underset{\sim}{x}},\rho'';\underset{\sim}{x}_0'') \triangleq \underset{\sim}{f}(\bar{\underset{\sim}{x}}) + (\rho''-1)\,\underset{\sim}{f}(\underset{\sim}{x}_0'') = \underset{\sim}{0},\ \rho'' \neq 1 \tag{38}$$

Subtracting Eq. (38) from Eq. (37), we obtain

$$(\rho'-1)\,\underset{\sim}{f}(\underset{\sim}{x}_0') - (\rho''-1)\,\underset{\sim}{f}(\underset{\sim}{x}_0'') = \underset{\sim}{0} \tag{39}$$

or

$$\underset{\sim}{f}(\underset{\sim}{x}_0') = \frac{(\rho''-1)}{(\rho'-1)}\,\underset{\sim}{f}(\underset{\sim}{x}_0'') \tag{40}$$

But this contradicts our hypothesis that $\underset{\sim}{f}(\underset{\sim}{x}_0') \neq k\underset{\sim}{f}(\underset{\sim}{x}_0'')$. □

Observe that proposition 3 does not assert that each solution curve must necessarily pass through <u>all</u> solutions of $\underset{\sim}{f}(\underset{\sim}{x}) = \underset{\sim}{0}$. It only asserts that each point of intersection between two solution curves is also a solution of $\underset{\sim}{f}(\underset{\sim}{x}) = \underset{\sim}{0}$. In fact, as will be shown in the next section,

it is possible for a solution curve $\Gamma(\underset{\sim}{x}_0)$ to pass through only some of the solutions of $\underset{\sim}{f}(\underset{\sim}{x}) = \underset{\sim}{0}$. This will occur, for example, when the solution curve $\hat{\underset{\sim}{f}}(\underset{\sim}{x},\rho;\ \underset{\sim}{x}_0) = 0$ consists of several disconnected branches, such as the ones depicted in Fig. 1. However, it is also often possible to choose some initial vector $\underset{\sim}{x}_0$ such that the corresponding solution curve consists of only one contiguous branch. Hence, even though our algorithm will not guarantee that all solutions of $\underset{\sim}{f}(\underset{\sim}{x}) = \underset{\sim}{0}$ will be found for an arbitrary choice of $\underset{\sim}{x}_0$, a useful strategy that will usually succeed in finding most, if not all, solutions is simply to repeat the algorithm with several different initial vectors chosen around the boundary of the compact set D where the solutions are being sought. Moreover, on the strength of proposition 3, we know all solution curves must intersect at solutions of $\underset{\sim}{f}(\underset{\sim}{x}) = \underset{\sim}{0}$ and hence no extraneous solutions will ever be encountered. To illustrate this strategy, consider the hypothetical example shown in Fig. 5, where the solutions of $\underset{\sim}{f}(\underset{\sim}{x}) = \underset{\sim}{0}$ are to be found inside the compact domain D. Suppose we choose an initial point at the center of each boundary. A hypothetical solution curve $\Gamma(\underset{\sim}{x}'_0)$ is shown passing through solutions ②, ③, ④, ⑧ and ⑨, whereas that of $\Gamma(\underset{\sim}{x}''_0)$ is shown passing through solutions ①, ②, ③, ④, ⑤, ⑥, ⑦, ⑧ and ⑨. Another hypothetical solution curve $\Gamma(\underset{\sim}{x}'''_0)$ is shown passing through solutions ③, ⑤, ⑥ and ⑦, whereas that of $\Gamma(\underset{\sim}{x}''''_0)$ is shown passing through solutions ①, ②, ③, ④, ⑤, ⑥ and ⑦. Observe that the union of all intersection points of the two solution curves $\Gamma(\underset{\sim}{x}'_0)$ and $\Gamma(\underset{\sim}{x}''''_0)$ gives us a total of 9 solutions. There is of course no guarantee that all solutions will be found with this strategy. However, since our switching-parameter

algorithm is very efficient, we could often afford to repeat the algorithm with several initial points. The motivation being that each new solution curve might give rise to additional points of intersection.

V. SOLVING RESISTIVE NETWORKS WITH MULTIPLE SOLUTIONS VIA THE SWITCHING-PARAMETER ALGORITHM

We will now apply the switching-parameter algorithm to solve two basic problems associated with resistive networks having multiple solutions [1]; namely, the problem of finding the operating points, and the problem of finding driving-point or transfer characteristic curves. In both cases, we are concerned with networks containing non-monotonic voltage-controlled and current-controlled resistors. Since nodal analysis is no longer applicable for this class of networks, let us choose the more general tableau formulation given in [13]; namely,

$$\begin{bmatrix} \underset{\sim}{1} & -\underset{\sim}{A}^t & \underset{\sim}{0} \\ \underset{\sim}{K}_v & \underset{\sim}{0} & \underset{\sim}{K}_i \\ \underset{\sim}{0} & \underset{\sim}{0} & \underset{\sim}{A} \end{bmatrix} \begin{bmatrix} \underset{\sim}{V} \\ \underset{\sim}{V}_n \\ \underset{\sim}{I} \end{bmatrix} - \begin{bmatrix} \underset{\sim}{E} \\ \underset{\sim}{g}(\underset{\sim}{V},\underset{\sim}{I}) \\ \underset{\sim}{A}\underset{\sim}{J} \end{bmatrix} \triangleq \begin{bmatrix} \underset{\sim}{f}_\alpha(\underset{\sim}{V},\underset{\sim}{V}_n) \\ \underset{\sim}{f}_\beta(\underset{\sim}{V},\underset{\sim}{I}) \\ \underset{\sim}{f}_\gamma(\underset{\sim}{I}) \end{bmatrix} = \begin{bmatrix} \underset{\sim}{0} \\ \underset{\sim}{0} \\ \underset{\sim}{0} \end{bmatrix} \qquad (41)$$

where

$\underset{\sim}{V}$ is a b x 1 vector of branch voltages

$\underset{\sim}{E}$ is a b x 1 vector of voltage sources

$\underset{\sim}{I}$ is a b x 1 vector of branch currents

$\underset{\sim}{J}$ is a b x 1 vector of current sources

$\underset{\sim}{V}_n$ is an (n-1) x 1 vector of node-to-datum voltages

$\underset{\sim}{A}$ is the associated (n-1) x b reduced-incidence matrix, where b is the number of branches and n is the number of nodes.

$\underset{\sim}{K}_v$ and $\underset{\sim}{K}_i$ are b x b matrices for specifying the constitutive relation of the linear elements

$\underset{\sim}{g}(\underset{\sim}{V},\underset{\sim}{I})$ is a b x 1 vector whose j-th component is either a nonlinear function if the corresponding element is a nonlinear resistor, or

is equal to zero, if otherwise.

Observe that the first and third equations $\underset{\sim}{f}_{\alpha}(\underset{\sim}{V},\underset{\sim}{V}_n) = \underset{\sim}{0}$ and $\underset{\sim}{f}_{\gamma}(\underset{\sim}{I}) = \underset{\sim}{0}$ are actually linear equations representing KVL and KCL, respectively. The second equation $\underset{\sim}{f}_{\beta}(\underset{\sim}{V},\underset{\sim}{I}) = \underset{\sim}{0}$ represents the elements constitutive relations and is in a form which includes both voltage- and current-controlled resistors. We will define two <u>augmented</u> systems of equations, one is better suited for finding the operating points, while the other is more suited for finding driving-point and transfer characteristic curves.

A. <u>Augmented System for Finding Operating Points</u>

Let us introduce a parameter ρ as in Eq. (6) and recast Eq. (41) as follows:

$$\begin{bmatrix} \underset{\sim}{f}_{\alpha}(\underset{\sim}{V},\underset{\sim}{V}_n) \\ \underset{\sim}{f}_{\beta}(\underset{\sim}{V},\underset{\sim}{I}) \\ \underset{\sim}{f}_{\gamma}(\underset{\sim}{I}) \end{bmatrix} + (\rho-1) \begin{bmatrix} \underset{\sim}{f}_{\alpha}(\underset{\sim}{V}^{(0)},\underset{\sim}{V}_n^{(0)}) \\ \underset{\sim}{f}_{\beta}(\underset{\sim}{V}^{(0)},\underset{\sim}{I}^{(0)}) \\ \underset{\sim}{f}_{\gamma}(\underset{\sim}{I}^{(0)}) \end{bmatrix} \triangleq \begin{bmatrix} \hat{\underset{\sim}{f}}_{\alpha}(\underset{\sim}{V},\underset{\sim}{V}_n,\rho) \\ \hat{\underset{\sim}{f}}_{\beta}(\underset{\sim}{V},\underset{\sim}{I},\rho) \\ \hat{\underset{\sim}{f}}_{\gamma}(\underset{\sim}{I},\rho) \end{bmatrix} = \begin{bmatrix} \underset{\sim}{0} \\ \underset{\sim}{0} \\ \underset{\sim}{0} \end{bmatrix} \quad (42)$$

where $\underset{\sim}{V}^{(0)}$, $\underset{\sim}{V}_n^{(0)}$ and $\underset{\sim}{I}^{(0)}$ denote an arbitrary initial guess. The associated system of linear equations corresponding to Eqs. (17)-(18) is given by:

$$\begin{bmatrix} \underset{\sim}{1} & -\underset{\sim}{A}^t & \underset{\sim}{0} & \underset{\sim}{f}_\alpha(\underset{\sim}{V}^{(0)},\underset{\sim}{V}_n^{(0)}) \\ \underset{\sim}{K}_v - \left.\frac{\partial \underset{\sim}{g}(\underset{\sim}{V},\underset{\sim}{I})}{\partial \underset{\sim}{V}}\right|_{(\underset{\sim}{V}^{(j)},\underset{\sim}{I}^{(j)})} & \underset{\sim}{0} & \underset{\sim}{K}_i - \left.\frac{\partial \underset{\sim}{g}(\underset{\sim}{V},\underset{\sim}{I})}{\partial \underset{\sim}{I}}\right|_{(\underset{\sim}{V}^{(j)},\underset{\sim}{I}^{(j)})} & \underset{\sim}{f}_\beta(\underset{\sim}{V}^{(0)},\underset{\sim}{I}^{(0)}) \\ \underset{\sim}{0} & \underset{\sim}{0} & \underset{\sim}{A} & \underset{\sim}{f}_\gamma(\underset{\sim}{I}^{(0)}) \end{bmatrix} \begin{bmatrix} \underset{\sim}{V}^{(j+1)} - \underset{\sim}{V}^{(j)} \\ \underset{\sim}{V}_n^{(j+1)} - \underset{\sim}{V}_n^{(j)} \\ \underset{\sim}{I}^{(j+1)} - \underset{\sim}{I}^{(j)} \\ \rho^{(j+1)} - \rho^{(j)} \end{bmatrix} = - \begin{bmatrix} \hat{\underset{\sim}{f}}_\alpha(\underset{\sim}{V}^{(j)},\underset{\sim}{I}^{(j)},\rho^{(j)}) \\ \hat{\underset{\sim}{f}}_\beta(\underset{\sim}{V}^{(j)},\underset{\sim}{I}^{(j)},\rho^{(j)}) \\ \hat{\underset{\sim}{f}}_\gamma(\underset{\sim}{I}^{(j)},\rho^{(j)}) \end{bmatrix} \tag{43}$$

$$\operatorname{sgn}\left(\left.\frac{dx_k}{ds}\right|_{x_k = x_k^{(j+1)}} \right) \left(x_k^{(j+1)} - x_k^{(j)}\right) = h \tag{44}$$

where the variable $x_k \in \{\underset{\sim}{V}, \underset{\sim}{V}_n, \underset{\sim}{I}, \rho\}$ is chosen at each integration step such that

$$|\Delta x_k| = \max \{|\Delta V_i|, |\Delta V_{n_i}|, |\Delta I_i|, |\Delta \rho|\} \tag{45}$$

Solving Eqs. (43)-(44) via the switching-parameter algorithm, we obtain all solutions lying on the solution curve corresponding to the initial point $(\underset{\sim}{V}^{(0)}, \underset{\sim}{V}_n^{(0)}, \underset{\sim}{I}^{(0)}, \rho^{(0)})$. Observe that even though the dimension of the matrix in Eq. (43) is much larger than the corresponding nodal admittance matrix, it is extremely sparse and may be efficiently computed using sparse-matrix techniques [13].

Example 2.

Find the operating points of the circuit shown in Fig. 6(a) where the constitutive relations of the two tunnel diodes are shown in Figs. 6(b) and (c), respectively.

For this simple circuit, the following equations can be obtained by inspection:

$$f_1(V_1, V_2) \triangleq E - Rg_1(V_1) - (V_1 + V_2) = 0 \tag{46}$$

$$f_2(V_1, V_2) \triangleq g_1(V_1) - g_2(V_2) = 0 \tag{47}$$

where

$$g_1(V_1) \triangleq 2.5\, V_1^3 - 10.5\, V_1^2 + 11.8\, V_1 \tag{48}$$

$$g_2(V_2) \triangleq 0.43\, V_2^3 - 2.69\, V_2^2 + 4.56\, V_2 \tag{49}$$

The augmented system of equations is given by

$$\hat{f}_1(V_1,V_2,\rho) \triangleq f_1(V_1,V_2) + (\rho-1)\, f_1(V_1^{(0)},V_2^{(0)}) = 0 \qquad (50)$$

$$\hat{f}_2(V_1,V_2,\rho) \triangleq f_2(V_1,V_2) + (\rho-1)\, f_2(V_1^{(0)},V_2^{(0)}) = 0 \qquad (51)$$

For illustrative purposes, the following <u>four</u> initial points were chosen:

1. $(V_1^{(0)},V_2^{(0)},\rho^{(0)}) = (0,0,0)$ 2. $(V_1^{(0)},V_2^{(0)},\rho^{(0)}) = (3,0,0)$

2. $(V_1^{(0)},V_2^{(0)},\rho^{(0)}) = (0,3,0)$ 4. $(V_1^{(0)},V_2^{(0)},\rho^{(0)}) = (3,3,0)$

The corresponding solution curves are obtained by the switching-parameter algorithm and are shown in Fig. 6(d). Notice that these solution curves all intersect each other at the plane $\rho = 1$ and it follows from <u>Proposition 3</u> that these points of intersection are the <u>operating points</u>. The same set of operating points can be obtained by projecting the solution curves onto the $V_1 - V_2$ plane as shwon in Fig. 6(e) and then locating those points with $\rho = 1$. Observe that the <u>first</u> and <u>third</u> solution curves pass through only 5 operating points (①, ②, ③, ⑥ and ⑨) whereas the <u>second</u> and <u>fourth</u> solution curves pass through all 9 operating points. Also shown in Fig. 6(e) are dotted lines indicating the points where the Jacobian matrix associated with Eqs. (48)-(49) is singular. Notice that our algorithm is applicable even though the solution curve passes through several points whose associated Jacobian matrix is not of full rank.

B. <u>Augmented System for Finding Driving-Point and Transfer Characteristic Plots</u>

Let N be a resistive nonlinear network containing in addition to fixed <u>internal</u> voltage and current sources, an input voltage V_{in} which

varies from $-E_1$ to E_2. The problem is to derive the relationship between the input current I_{in} and the input voltage V_{in}, or between some output voltage V_0 and the input voltage V_{in}. To solve this problem using the tableau formulation, let us decompose the voltage source vector $\underset{\sim}{E}$ in Eq. (41) as follows:

$$\underset{\sim}{E} = \lambda(\underset{\sim}{E}_{int} - \underset{\sim}{E}_1) + \rho(\underset{\sim}{E}_1 + \underset{\sim}{E}_2) \tag{52}$$

where

$$\underset{\sim}{E} \triangleq \begin{bmatrix} e_1 \\ e_2 \\ \vdots \\ e_{k-1} \\ e_k \\ e_{k+1} \\ \vdots \\ e_b \end{bmatrix}, \quad \underset{\sim}{E}_{int} \triangleq \begin{bmatrix} e_1 \\ e_2 \\ \vdots \\ e_{k-1} \\ 0 \\ e_{k+1} \\ \vdots \\ e_b \end{bmatrix}, \quad \underset{\sim}{E}_1 \triangleq \begin{bmatrix} 0 \\ 0 \\ \vdots \\ 0 \\ E_1 \\ 0 \\ \vdots \\ 0 \end{bmatrix}, \quad \underset{\sim}{E}_2 \triangleq \begin{bmatrix} 0 \\ 0 \\ \vdots \\ 0 \\ E_2 \\ 0 \\ \vdots \\ 0 \end{bmatrix} \tag{53}$$

where $e_1, e_2, \ldots, e_{k-1}, e_{k+1}, \ldots e_b$ denote the <u>internal</u> voltage sources, $e_k \triangleq V_{in}$ denotes the <u>input</u> voltage source, and where λ and ρ are two scalar parameters. Observe that when $\lambda = 1$, the internal sources are set at their full values. Observe also that when $\lambda = 1$ and $\rho = 0$, we have $V_{in} = -E_1$. Similarly, when $\lambda = 1$ and $\rho = 1$, we have $V_{in} = E_2$. Now, recast Eq. (41) as follows:

$$\begin{bmatrix} \underset{\sim}{1} & -\underset{\sim}{A}^t & \underset{\sim}{0} \\ \underset{\sim}{K}_v & \underset{\sim}{0} & \underset{\sim}{K}_i \\ \underset{\sim}{0} & \underset{\sim}{0} & \underset{\sim}{A} \end{bmatrix} \begin{bmatrix} \underset{\sim}{V} \\ \underset{\sim}{V}_n \\ \underset{\sim}{I} \end{bmatrix} - \begin{bmatrix} \lambda(\underset{\sim}{E}_{int} - \underset{\sim}{E}_1) + \rho(\underset{\sim}{E}_1 + \underset{\sim}{E}_2) \\ \underset{\sim}{g}(\underset{\sim}{V}, \underset{\sim}{I}) \\ \lambda \underset{\sim\sim}{A} \underset{\sim\sim}{J} \end{bmatrix} \triangleq \begin{bmatrix} \hat{\underset{\sim}{f}}_\alpha(\underset{\sim}{V}, \underset{\sim}{V}_n, \lambda, \rho) \\ \hat{\underset{\sim}{f}}_\beta(\underset{\sim}{V}, \underset{\sim}{I}, \lambda, \rho) \\ \hat{\underset{\sim}{f}}_\gamma(I, \lambda) \end{bmatrix} = \begin{bmatrix} \underset{\sim}{0} \\ \underset{\sim}{0} \\ \underset{\sim}{0} \end{bmatrix} \tag{54}$$

Suppose we set $\rho = 0$ in Eq. (54) and trace the solution curve via the switching-parameter algorithm from $\lambda = 0$ to $\lambda = 1$.[5] When $\lambda = 0$ and $\rho = 0$, all sources, including the input voltage source, are set to zero. If all resistors inside N are passive, which is usually the case for most practical circuits, then the solution to Eq. (54) when $\lambda = \rho = 0$ is simply $\underset{\sim}{V} = \underset{\sim}{0}$, $\underset{\sim}{V}_n = \underset{\sim}{0}$ and $\underset{\sim}{I} = \underset{\sim}{0}$. Hence, by holding $\rho = 0$, we can apply the switching-parameter algorithm to solve for the solution curve of the system of equations

$$\left.\begin{aligned} \hat{\underset{\sim}{f}}_\alpha(\underset{\sim}{V},\underset{\sim}{V}_n,\lambda,0) &= \underset{\sim}{0} \\ \hat{\underset{\sim}{f}}_\beta(\underset{\sim}{V},\underset{\sim}{I},\lambda,0) &= \underset{\sim}{0} \\ \hat{\underset{\sim}{f}}_\gamma(\underset{\sim}{I},\lambda) &= \underset{\sim}{0} \end{aligned}\right\} \tag{55}$$

which passes through the initial point $Q(\lambda = 0)$ at $(\underset{\sim}{V}^{(0)},\underset{\sim}{V}_n^{(0)},\lambda^{(0)},\rho^{(0)}) = (\underset{\sim}{0},\underset{\sim}{0},0,0)$. Let $Q(\lambda = 1)$ be the point on this solution curve corresponding to $\lambda = 1$. Observe that the solution at $Q(\lambda = 1)$ corresponds to the case when all internal sources are set to their full values and when the input voltage is set to $V_i = -E_1$. Now, apply the switching-parameter algorithm once again to trace the solution curve of the system

$$\left.\begin{aligned} \hat{\underset{\sim}{f}}_\alpha(\underset{\sim}{V},\underset{\sim}{V}_n,1,\rho) &= \underset{\sim}{0} \\ \hat{\underset{\sim}{f}}_\beta(\underset{\sim}{V},\underset{\sim}{I},1,\rho) &= \underset{\sim}{0} \\ \hat{\underset{\sim}{f}}_\gamma(\underset{\sim}{I},1) &= \underset{\sim}{0} \end{aligned}\right\} \tag{56}$$

which passes through the new initial point $Q(\lambda = 1)$. The resulting

[5] The idea of tracing the driving-point and transfer characteristic curve via a solution curve is analogous to that proposed by Katzenelson [14] and Kuh and Hajj [15] for solving piecewise-linear resistive networks.

space curve is precisely the locus of the solutions with V_{in} changing from $-E_1$ to E_2. Hence, the I_{in} -vs.- V_{in} driving-point characteristic curve, or the V_0 -vs.- V_{in} transfer characteristic curve can be easily obtained by projecting this curve onto the I_{in} - V_{in} plane, or onto the V_0 - V_{in} plane. We will now present two examples to illustrate this two-step algorithm.

Example 3.

Find the V_0 -vs.- V_{in} transfer characteristic curve of the Schmitt Trigger circuit shown in Fig. 7(a) over the interval $0 \leq V_{in} \leq 5$ volts.

Since $V_{in} \geq 0$, it suffices to choose the transistor circuit model shown in Fig. 7(b), where the diodes are characterized by the usual exponential law [13]. Since there is only one internal voltage source, we can simplify the preceding algorithm by letting E_{int} and V_{in} assume the roles played by λ and ρ, respectively. Hence, setting first $V_{in} = 0$, we apply the switching-parameter algorithm with $E_{int} = 0$ as the initial point and trace the V_0 -vs.- E_{int} solution curve as shown in Fig. 7(c). Notice that this solution curve need only be traced up to $E_{int} = 10$ volts, the full supply voltage of the internal voltage source. This curve corresponds to $\lambda = 1$, $\rho = 0$ in Eq. (56). Hence, at $E_{int} = 10$ volts, we found $V_0 = 6.7$ volts -- the initial point for the desired solution curve. With E_{int} set at 10 volts, we apply the switching-parameter algorithm once again with $V_0 = 6.7$ volts as the initial point, and obtain the V_0 -vs.- V_{in} solution curve shown in Fig. 7(d). Observe that this transfer characteristic curve is a multivalued function of V_{in} and could not have been obtained by

conventional methods. The switching-parameter algorithm essentially chooses V_{in} as the independent variable until $V_{in} = 3.56$ volts, when it switches <u>automatically</u> to V_0 as the independent variable. When the solution curve reaches $V_0 = 10$ volts, the algorithm switches automatically back to V_{in} as the independent variable.

<u>Example 4</u>.

Consider the circuit shown in Fig. 6(a) which we redraw as shown in Fig. 8(a). The objective here is to derive the V_1 -vs.- V_{in} and the V_2 -vs.- V_{in} transfer characteristic curves over the interval $0 \leq V_{in} \leq 50$ volts. Since this circuit has no internal sources, we have $\underset{\sim}{E}_{int} = \underset{\sim}{0}$ and the first part of the preceding algorithm need not be carried out. Applying the switching-parameter algorithm with $(V_1,V_2,V_{in}) = (0,0,0)$, we obtain the solution curve Γ_1 shown in Fig. 8(b). Observe that Γ_1 intersects the vertical plane through $V_{in} = 30$ volts at five points; namely, ①, ②, ③, ④ and ⑤. The (V_1,V_2) coordinates of these five points coincide with those of the five operating points found earlier in Fig. 6(e) along the solution curve through $(V_1,V_2) = (0,0)$, as they should. One limitation of this algorithm is that if the transfer characteristic curve consists of more than one separate branches, only that branch passing through the initial point corresponding to $\rho = 0$ in Eq. (54) will be found. In this particular example, the transfer characteristic curve actually consists of two separate branches. To obtain the second branch, a point on it must first be found. Hence, returning to example 2, we found the circuit has nine operating points when $V_{in} = 30$ volts, five of them have already been found earlier to lie on one branch of the solution curve

Γ_1. Hence, any one of the remaining four operating points may be chosen as the next initial point. Applying the switching-parameter algorithm once again with operating point (8) at $(V_1,V_2) = (2.289,1.856)$ as the new initial point, we obtain the second branch Γ_2 of the solution curve as shown in Fig. 8(b). To obtain the V_1 -vs.- V_{in} transfer characteristic curve, we simply project the two solution curves Γ_1 and Γ_2 onto the $V_1 - V_{in}$ plane. Similarly, the V_2 -vs.- V_{in} transfer characteristic curve is obtained by projecting Γ_1 and Γ_2 onto the $V_2 - V_{in}$ plane.

VI. CONCLUDING REMARKS

A new algorithm for obtaining the multiple solutions of a system of nonlinear algebraic equations has been presented. This algorithm consists of tracing the solution curves of an associated system of differential equations whose independent variable may switch from one variable to another during each integration step. The switching occurs whenever the solution curve changes direction, thereby requiring the choice of a new independent variable. This switching operation is implemented automatically at each integration step by choosing that variable $x_k \in \{x_1, x_2, \ldots, x_n, \rho\}$ which varies most rapidly during the preceding integration step as the independent variable. Although any numerical integration method may presumably be used to trace the solution curve, it is shown that the choice of the Forward Euler predictor and Newton-Raphson corrector leads to an extremely efficient algorithm which can be easily programmed. In fact, the algorithm consists of simply solving, recursively, a system of linear algebraic equations given by Eqs. (17)-(18) (with appropriate parameter up-dating) three times per integration step: The first time corresponds to that of integrating the associated system of differential equations by the Forward Euler method with a pre-set step size h; the next two times correspond to a correction of this predicted value by two Newton-Raphson iterations and are implemented by simply solving Eqs. (17)-(18) with $h = 0$. A uniform step size has so far been used in this study. It is conceivable that a variable step size may be advantageous provided that an efficient method for estimating the local truncation error can be developed [13].

The switching-parameter algorithm can also be used effectively to

obtain at least one branch of a multivalued driving-point or transfer characteristic curve of a resistive nonlinear network. In the special case where the associated characteristic curve is a single-valued function of an input voltage V_{in}, we can simply choose V_{in} as the independent variable and no parameter switching is necessary. In particular, if we write the associated nonlinear equation by

$$\underset{\sim}{f}(\underset{\sim}{x},y) = \underset{\sim}{0} \tag{57}$$

where $y \triangleq V_{in}$ and $\underset{\sim}{x} \in \mathbb{R}^n$ denote the remaining network variables, then the driving-point or transfer-characteristic curve can be obtained by simply integrating the associated system of differential equations

$$\frac{d\underset{\sim}{x}}{dy} = -\left(\frac{\partial \underset{\sim}{f}}{\partial \underset{\sim}{x}}\right)^{-1}\left(\frac{\partial \underset{\sim}{f}}{dy}\right) \tag{58}$$

In this case, it may be more efficient to choose a multi-step implicit algorithm -- such as Adams-Moulton or Gear's algorithm [13].

The switching-parameter algorithm presented in this paper can of course be used to trace the solution curve of any "well-posed" system of "n" equations in (n+1) unknowns. In particular, this algorithm may be applied to trace the solution curve associated with Shinohara's [10] or Chao's [12] method since in either case the solution curve associated with the first (n-1) equations in n unknowns must be found.

The switching-parameter algorithm does have two serious problems. The first problem has already been encountered in Example 4, where the solution curve consists of more than one separate branch. In this case, only the branch passing through the initial point will be found. This

problem also occurs in all other known algorithms for finding multiple solutions and no panacea seems to be forthcoming. The second problem corresponds to the case when a solution tends toward a limit cycle in $\mathbb{R}^2$, or toward a periodic orbit in $\mathbb{R}^n$, which fails to intersect with the hyperplane $\rho = \rho^*$ in Fig. 1. This situation may arise when the rank of the $n \times (n+1)$ Jacobian matrix of $\hat{f}(x,\rho)$ is less than n along the solution curve. Although this problem can sometimes be overcome by choosing another initial point so that the associated solution curve will intersect the $\rho = \rho^*$ hyperplane, no systematic method is yet available for choosing such initial points.

In conclusion, the classical problem of finding the set of all multiple solutions remains unsolved. The switching-parameter algorithm represents by far the most efficient method for finding some, if not all, of the solutions.

ACKNOWLEDGEMENT

The authors would like to thank Professor Y-F Lam and Mr. N. N. Wang from the University of California, Berkeley, for their comments on an earlier version of this manuscript.

REFERENCES

1. Chua, L.O., Introduction to Nonlinear Network Theory, McGraw-Hill, New York, N.Y., 1969.

2. Hayashi, C., Nonlinear Oscillation in Physical Systems, McGraw-Hill, New York, N.Y., 1964.

3. Ortega, J.M. and W.C. Rheinboldt, Iterative Solution of Nonlinear Equations in Several Variables, Academic Press, New York, N.Y., 1970.

4. Chua, L.O., "Efficient Computer Algorithms for Piecewise-Linear Analysis of Resistive Nonlinear Networks", IEEE Trans. on Circuit Theory, Vol. 18, No. 1, January 1971, pp. 73-85.

5. Chien, M.J. and E.S. Kuh, "Solving Piecewise-Linear Equations for Resistive Networks: Theory and Algorithms", ERL Memorandum #M471, University of California, Berkeley, September 1974.

6. Davidenko, D.F., "On a New Method for Numerical Solution of Systems of Nonlinear Equations", Dokl. Akad. Nauk. SSSR, Vol. 88, 1953, pp. 601-602.

7. Yakovlav, M.N., "The Solution of Systems of Nonlinear Equations by a Method of Differentiation with Respect to a Parameter", U.S.S.R., Comput. Math. and Math. Phys., Vol. 4, 1964, pp. 146-149.

8. Meyer, G.H., "On Solving Nonlinear Equations with a One-Parameter Operator Imbedding", SIAM J. Numer. Analy., Vol. 5, 1968, pp. 739-752.

9. Boggs, P.T., "The Solution of Nonlinear Systems of Equations by A-Stable Integration Techniques", SIAM J. Numer. Analy., Vol. 8, No. 4, 1971, pp. 767-785. Also Ph.D. Dissertation, Cornell University, 1970.

10. Shinohara, Y., "A Geometric Method of Numerical Solution of Nonlinear Equation and Error Estimation by Urabe's Proposition", RIMS, Kyoto

University, Vol. 5, No. 1, 1965, pp. 1-9.

11. Branin, F.H., Jr., "Widely Convergent Method for Finding Multiple Solution of Simultaneous Nonlinear Equations", IBM J. of Res. and Dev., Vol. 16, No. 5, September 1972, pp. 504-522.

12. Chao, K.S., Lin D.K. and Pan C.T., "A Systematic Search Method for Obtaining Multiple Solutions of Simultaneous Nonlinear Equations", Proc. of the 1974 International Symposium on Circuit and Systems, San Francisco, Ca., pp. 27-31.

13. Chua, L.O. and P-M Lin, Computer-Aided Analysis of Electronic Circuits: Algorithms and Computation Techniques, Prentice-Hall, Englewood Cliffs, N.J., 1975.

14. Katzenelson, J., "An Algorithm for Solving Nonlinear Resistive Networks", Bell Systems Tech. J., Vol. 44, Oct. 1965, pp. 1605-1620.

15. Kuh, E.S. and I. Hajj, "Nonlinear Circuit Theory -- Resistive Networks", Proc. of the IEEE, Vol. 59, 1971, pp. 340-355.

FIGURE CAPTIONS

Fig. 1. A geometrical interpretation showing two space curves passing through the initial points $\underset{\sim}{x}_0^{(1)}$ and $\underset{\sim}{x}_0^{(2)}$ at $\rho = \rho_0$ and intersecting the hyperplane $\rho = \rho^*$ at six solution points $x^{*(1)}, x^{*(2)}, \ldots, x^{*(6)}$.

Fig. 2. A typical space curve may be partitioned into the union of several segments, each one parametrized by a separate parameter.

Fig. 3. The flow chart for implementing the switching-parameter algorithm.

Fig. 4. An example showing a solution curve containing nine solutions, each one identified by the parameter value $\rho = 1$.

Fig. 5. An example showing four hypothetical solution curves originating from four uniformly-spaced initial points. The union of all intersecting points constitute the solutions.

Fig. 6. A nonlinear circuit having nine distinct solutions obtained by the switching-parameter algorithm.

Fig. 7. A Schmitt-Trigger circuit and its multivalued V_0 -vs.- V_{in} transfer characteristic curve.

Fig. 8. A nonlinear circuit exhibiting two separate solution curves.

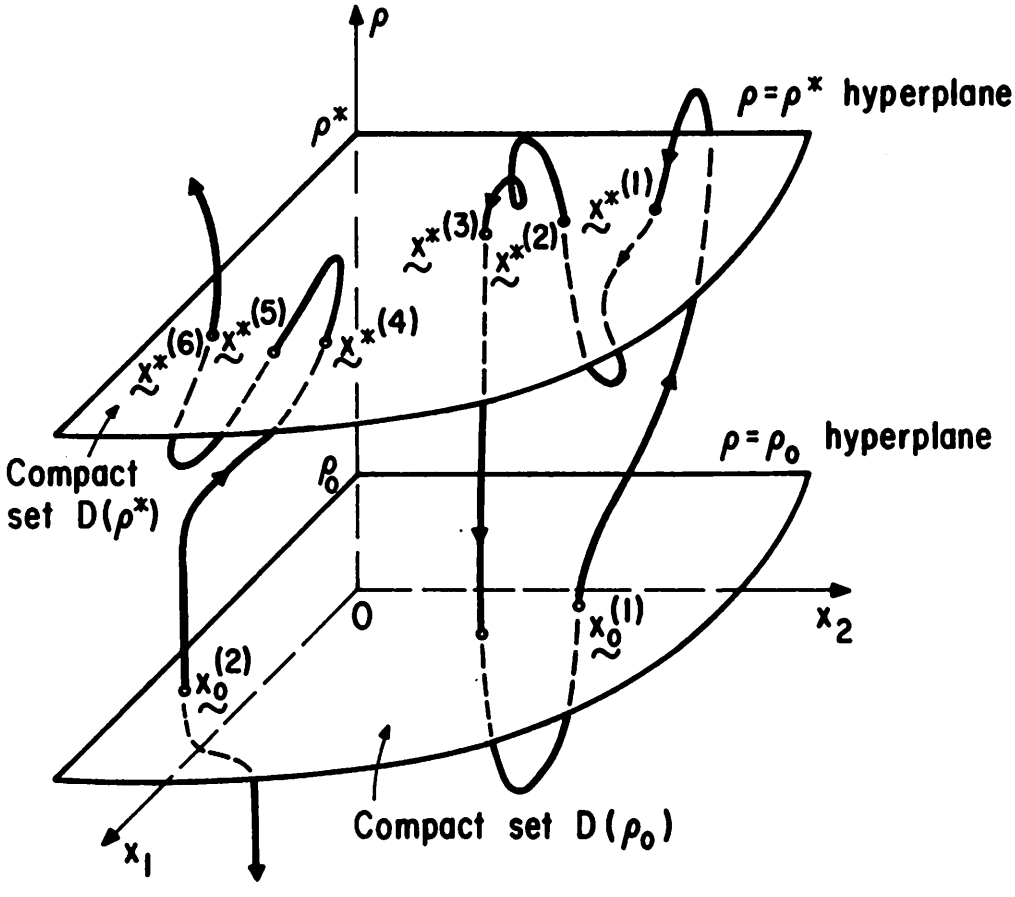

Fig. 1. A geometrical interpretation showing two space curves passing through the initial points $\underset{\sim}{x}_0^{(1)}$ and $\underset{\sim}{x}_0^{(2)}$ at $\rho = \rho_0$ and intersecting the hyperplane $\rho = \rho^*$ at six solution points $x^{*(1)}, x^{*(2)}, \ldots, x^{*(6)}$.

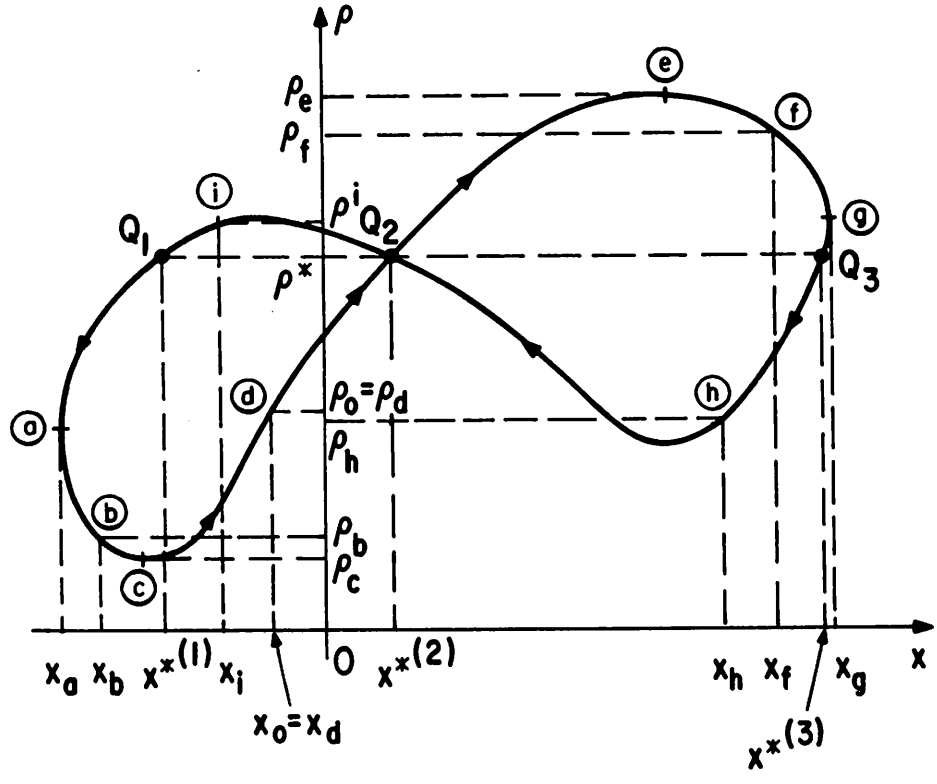

Fig. 2. A typical space curve may be partitioned into the union of several segments, each one parametrized by a separate parameter.

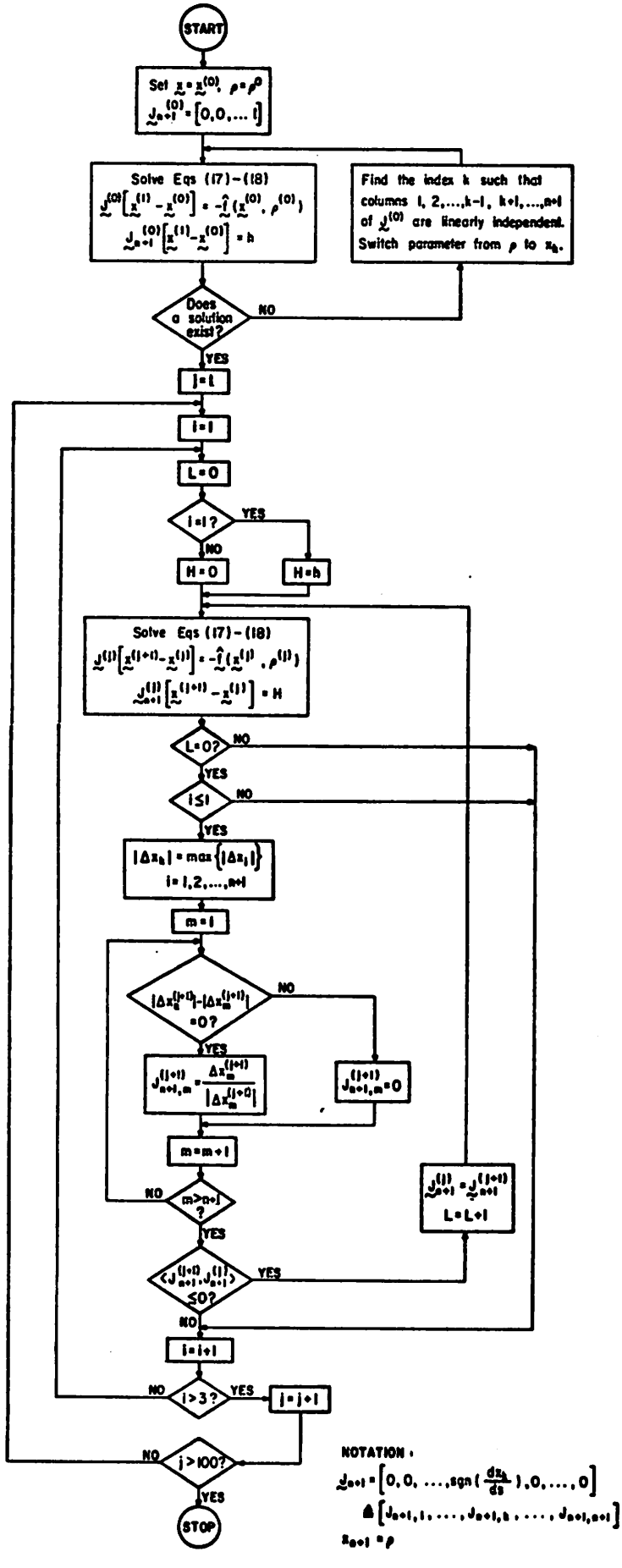

Fig. 3. The flow chart for implementing the switching-parameter algorithm.

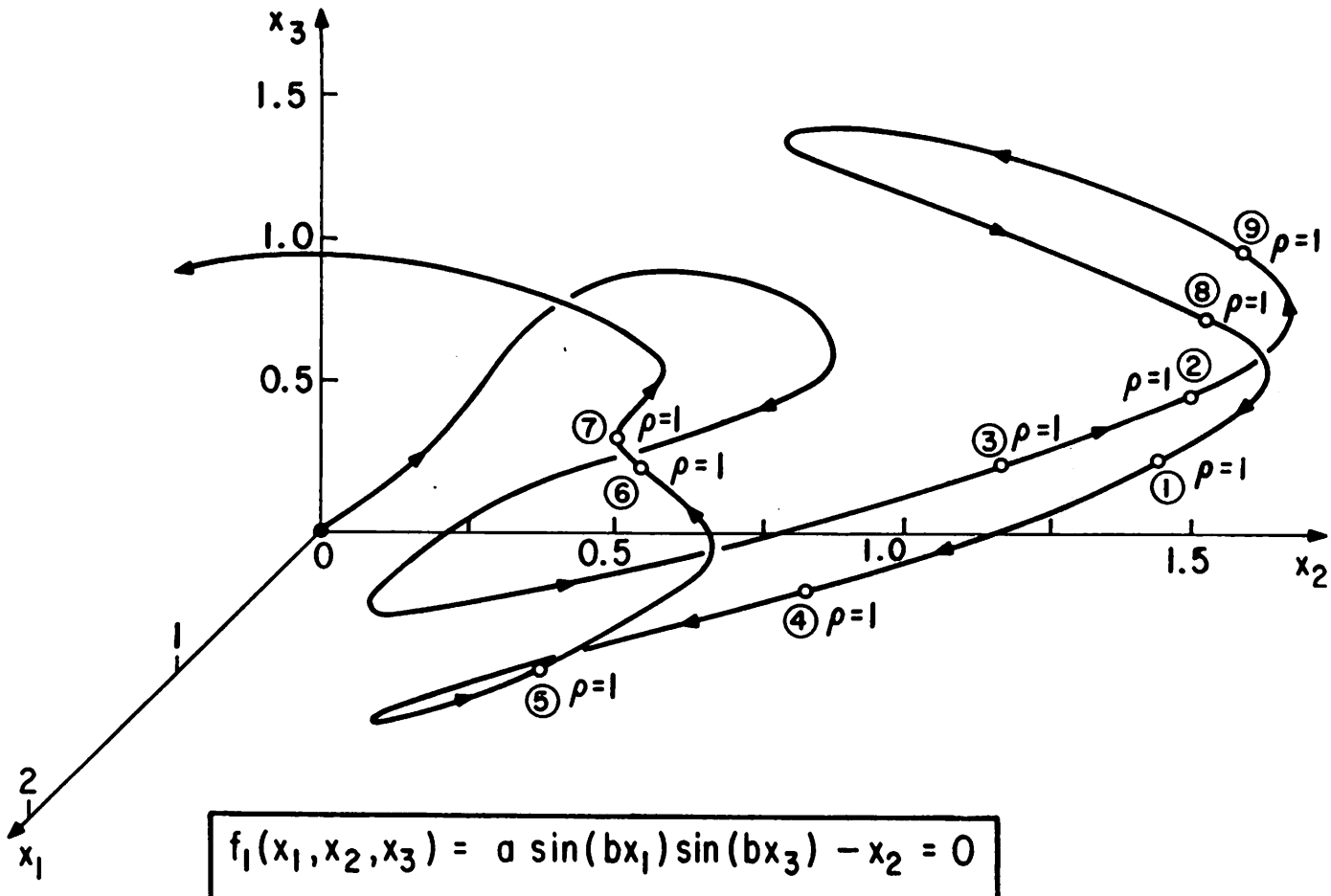

$$f_1(x_1, x_2, x_3) = a \sin(bx_1)\sin(bx_3) - x_2 = 0$$

$$f_2(x_1, x_2, x_3) = c - dx_3 + ex_2 \sin(fx_3) - x_1 = 0$$

$$f_3(x_1, x_2, x_3) = g + hx_2 \sin(kx_1) - x_3 = 0$$

The parameters are:

$a=2$, $b=0.4\pi$, $c=2.5$, $d=1$

$e=0.75$, $f=2\pi$, $g=1$, $h=0.8$, $k=2\pi$

The solutions are:

① (1.500, 1.809, 1.000)
② (0.991, 1.741, 0.926)
③ (0.951, 1.378, 0.663)
④ (1.575, 1.198, 0.566)
⑤ (1.879, 0.861, 0.524)
⑥ (2.027, 1.111, 1.152)
⑦ (2.048, 1.075, 1.257)
⑧ (1.451, 1.874, 1.454)
⑨ (1.054, 1.849, 1.494)

Fig. 4. An example showing a solution curve containing nine solutions, each one identified by the parameter value $\rho = 1$.

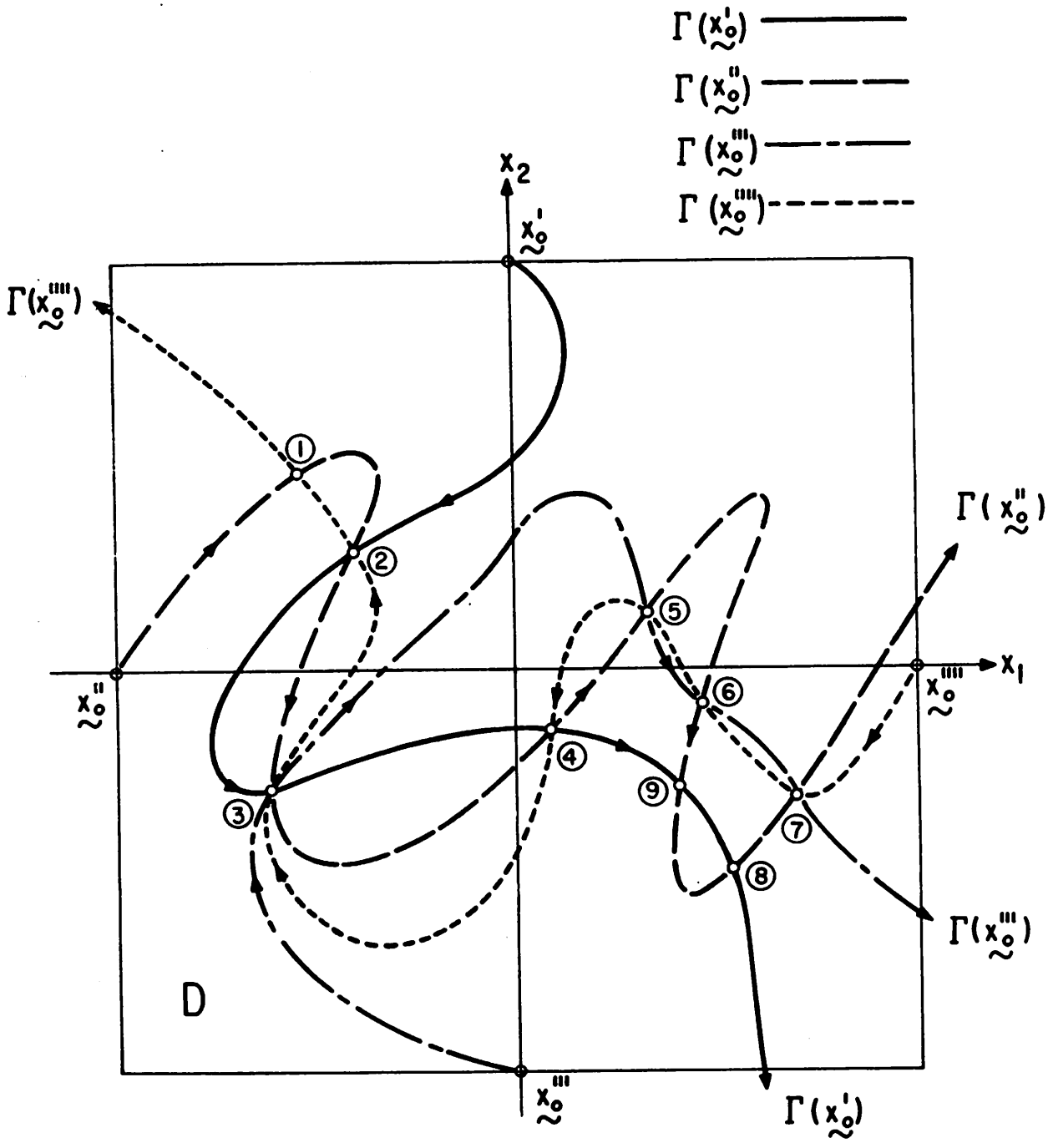

Fig. 5. An example showing four hypothetical solution curves originating from four uniformly-spaced initial points. The union of all intersecting points constitute the solutions.

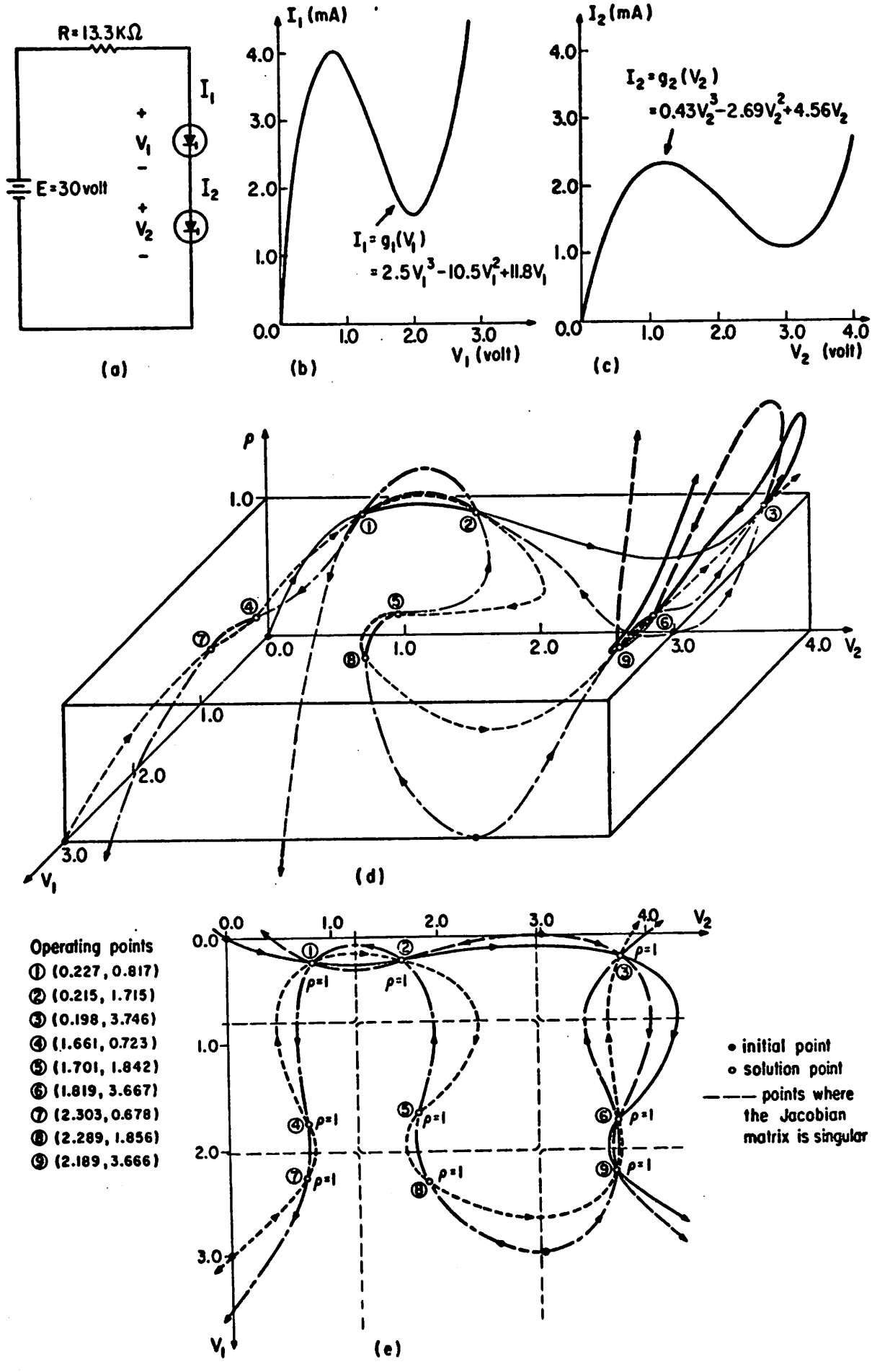

Fig. 6. A nonlinear circuit having nine distinct solutions obtained by the switching-parameter algorithm.

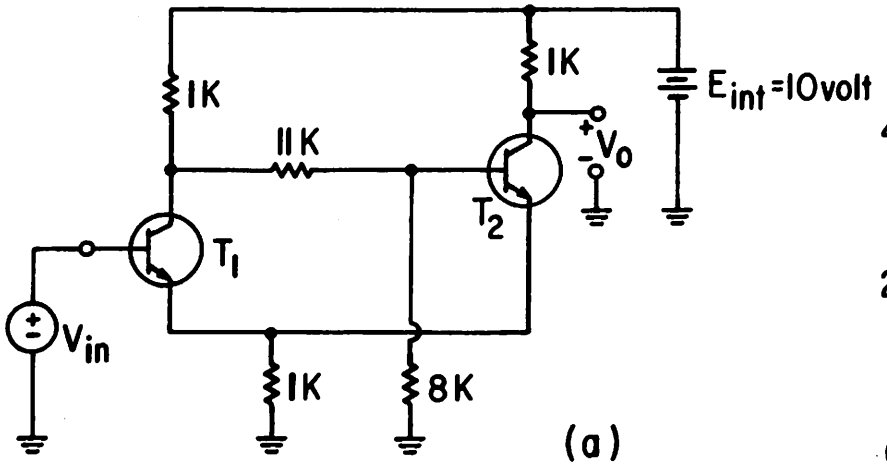

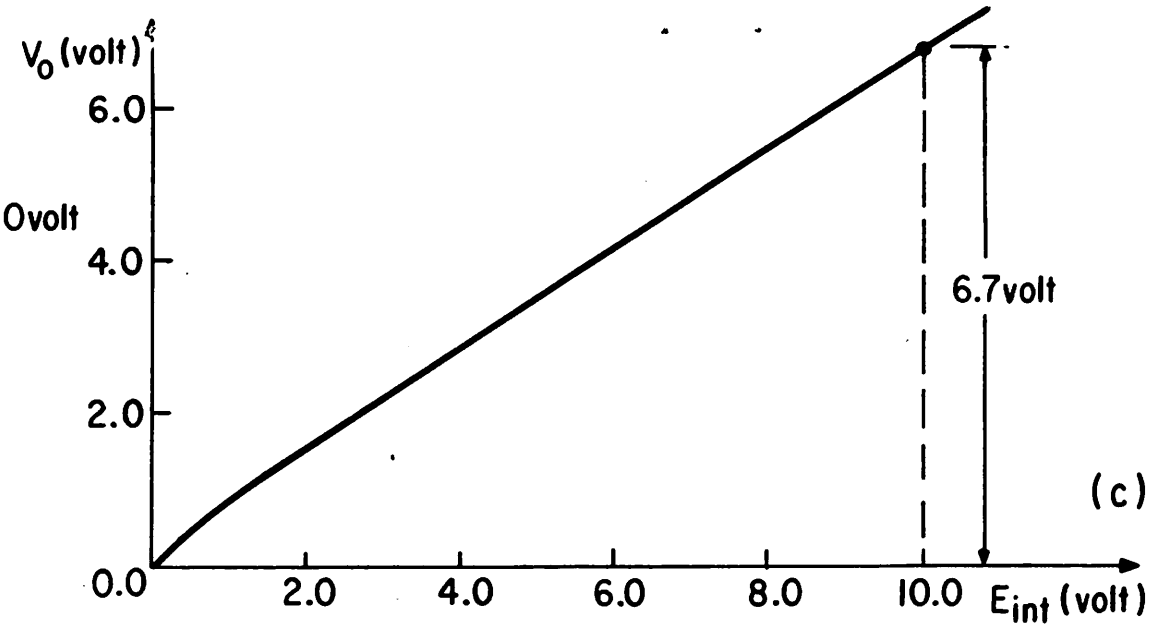

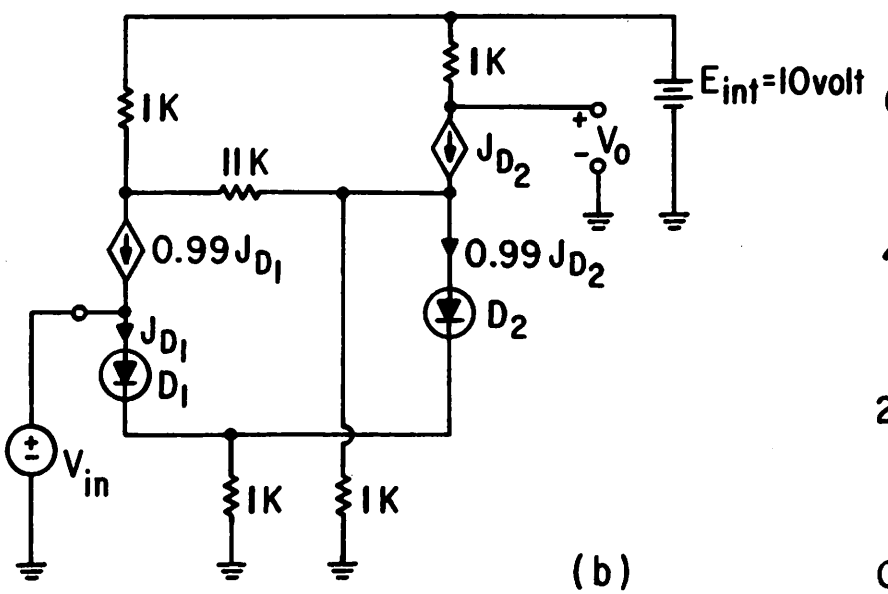

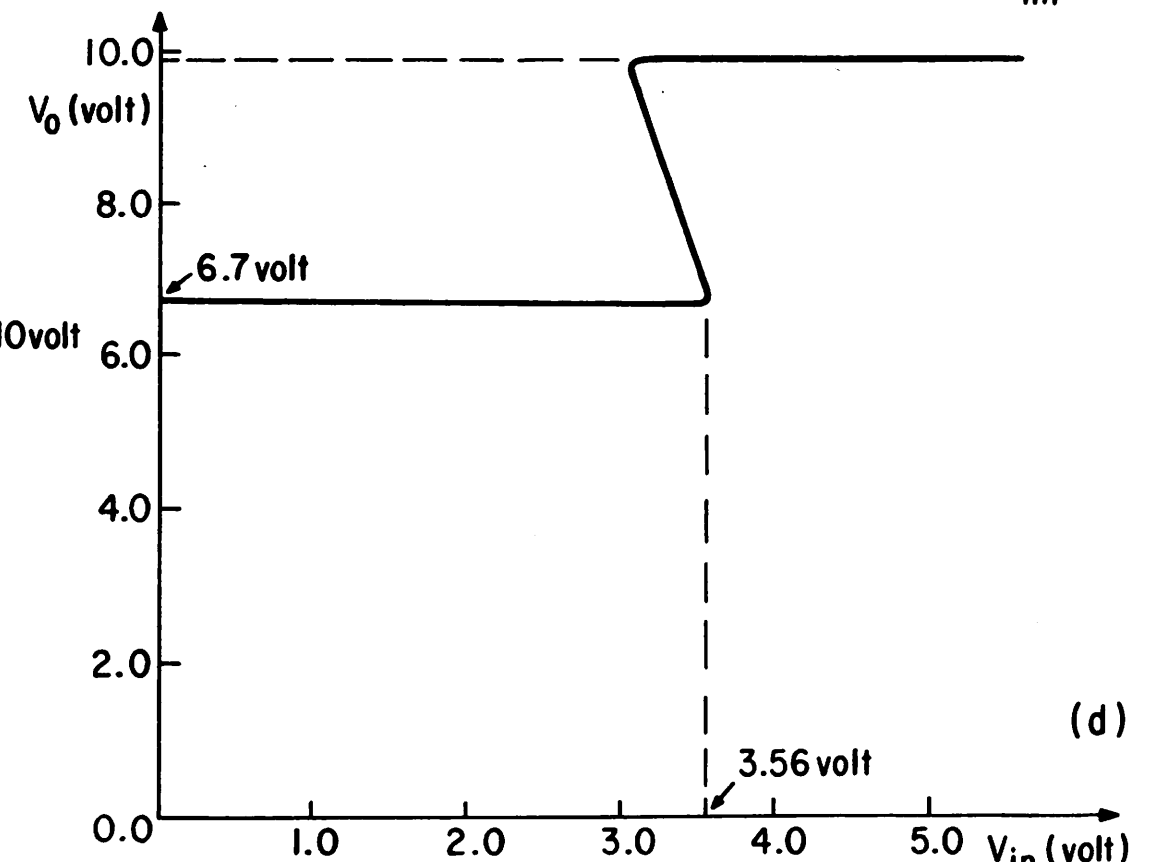

Fig. 7. A Schmitt-Trigger circuit and its multivalued V_o -vs.- V_{in} transfer characteristic curve.

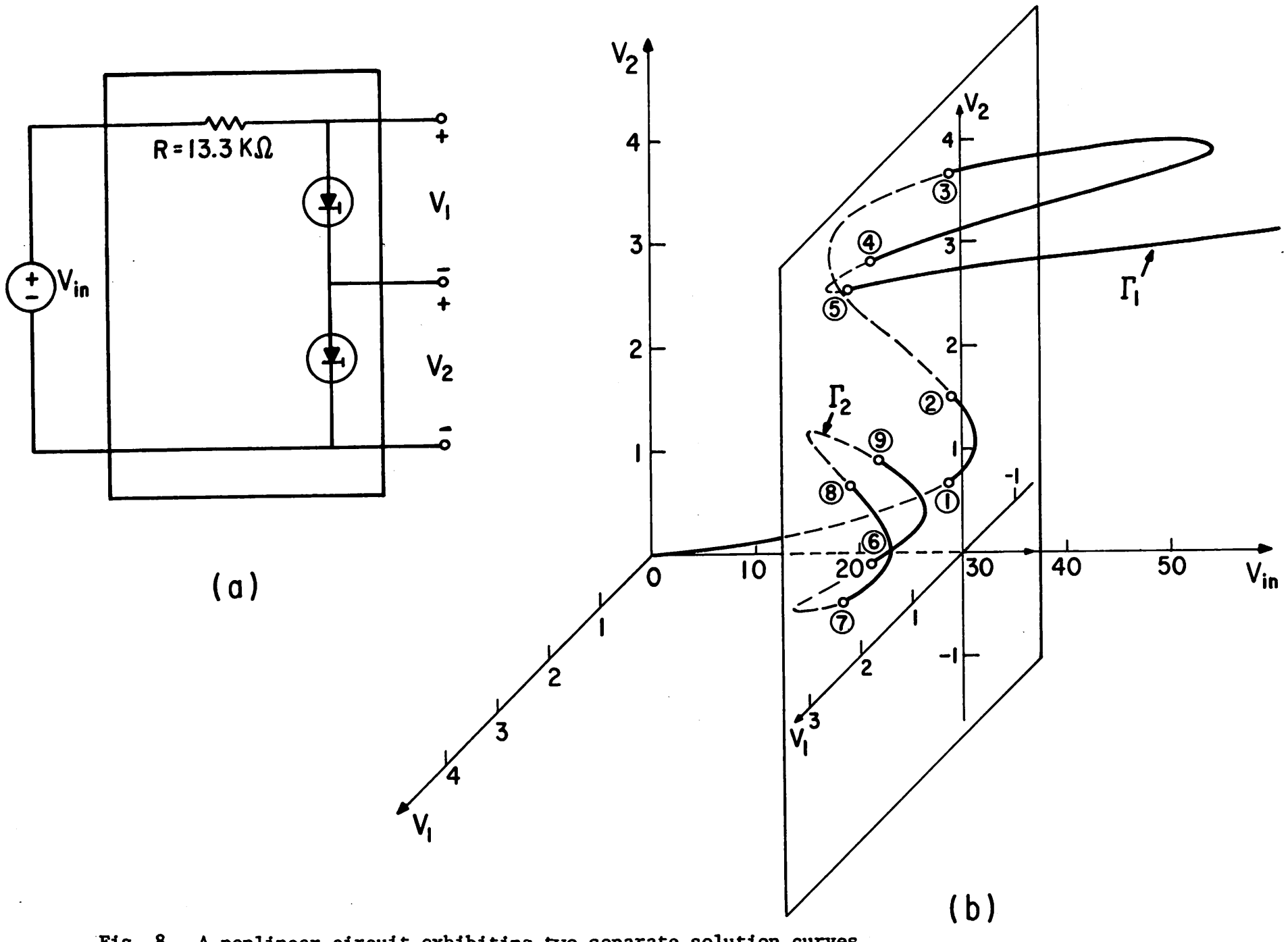

Fig. 8. A nonlinear circuit exhibiting two separate solution curves.